

VERTICAL DISTRIBUTION OF PARTICULATE MATTER IN A NEAR-HIGHWAY URBAN AREA

Piers MacNaughton
B.S. Environmental Engineering, 2012
Tufts University, School of Engineering
Department of Civil and Environmental Engineering

Senior Honors Thesis

Advisor: Professor John Durant

5/11/2012

Vertical Distribution of Particulate Matter in a Near-Highway Urban Area

by

Piers MacNaughton

Department of Civil and Environmental Engineering

Tufts University, Medford, MA, 02155

Abstract

This thesis describes research to better understand vertical profiles of particle number count and mass concentration of particles less than $2.5\text{ }\mu\text{m}$ in diameter ($\text{PM}_{2.5}$) near Interstate 93 in Boston, Massachusetts. These profiles can be used to help estimate particulate matter exposure to people who live or work several stories above ground-level. Although vertical profiles of particulate matter have been collected near major roadways in previous studies, none have been collected with as fine a spatial resolution and over as wide a range of meteorological conditions. The profiles were collected with a pulley system that lifted the instruments, leading to a continuous sampling of the vertical profiles. The vertical profiles are analyzed in conjunction with meteorological conditions, the source strength of the highway, and building density and height to obtain a qualitative assessment of each variable's effect on the magnitude and the slope of the particle profiles. The meteorological conditions considered in this thesis are wind direction and speed, temperature, and relative humidity on both a short and long timescale. The magnitude of the particle number count and $\text{PM}_{2.5}$ is primarily dependent on the source strength and the diurnal temperature cycle. The slope of the particle number count profile depends on the vertical temperature profile, whereas $\text{PM}_{2.5}$ remains constant with height. The profiles do not demonstrate a significant decline with height; therefore, exposure to particulate matter up to eight stories high should not be dismissed as an exposure pathway.

TABLE OF CONTENTS

1.0	INTRODUCTION	1
1.1	Background	1
1.2	Previous Vertical Profile Studies	2
1.3	Objectives	4
2.0	THEORY	5
2.1	Buoyancy.....	5
2.2	Turbulence.....	8
2.3	Particle Measurements	8
3.0	METHODS	10
3.1	Site Description	10
3.2	Experiment Procedure	12
3.2.1	Pulley System.....	12
3.2.2	Stationary Monitoring Box	14
3.2.3	Weather Balloon	14
3.3	Quality Assurance and Quality Control	14
3.3.1	Condensation Particle Counter	15
3.3.2	SidePak Aerosol Monitor.....	17
4.0	RESULTS AND DISCUSSION	18
4.1	Vertical Profile Gradient	18
4.1.1	Temperature	18
4.1.2	Particle Number Concentration.....	19
4.1.3	Particle Mass Concentration	21
4.2	Vertical Profile Magnitude.....	23
4.2.1	Wind Direction and Source Strength	23
4.2.2	Atmospheric Stability	26
4.3	Additional Variables	27
4.4	Long-term Air Quality	29
5.0	CONCLUSIONS.....	32
REFERENCES		
APPENDIX A – <i>Photo Log</i>		
APPENDIX B – <i>Experimental Procedure</i>		
APPENDIX C – <i>Example PNC Data Sheet and Macro Code</i>		

LIST OF FIGURES

Figure 1: Relationship of indoor air quality and outdoor air quality near I-93 (Fuller, 2011)	2
Figure 2: The effect of the actual lapse rate on vertical stability (Cooper and Alley, 2011).....	6
Figure 3: Typical diurnal variation of temperatures near the ground (Jacob, 1999)	7
Figure 4: Typical number and volume distributions of atmospheric particles (Seinfeld and Pandis, 2007).....	9
Figure 5: Site Locus	10
Figure 6: Aerial view of PSI	11
Figure 7: Street-view of I-93 and PSI with relevant structure heights looking north.....	12
Figure 8: CPC comparison test in the stationary monitoring box at PSI on 3/15/2012.....	15
Figure 9: CPC precision test in the laboratory at Tufts University on 4/5/2012	16
Figure 10: Vertical temperature profiles in the afternoon at PSI on 11/18/2011.....	18
Figure 11: Vertical Profiles of PNC and temperature at PSI from 11/18/11 to 12/16/11.....	20
Figure 12: Vertical Profiles in PNC and temperature at PSI from 1/20/12 to 2/15/12.....	21
Figure 13: Diurnal variations in $PM_{2.5}$ with respect to height at PSI from 11/18/11 to 2/15/12..	22
Figure 14: Extended $PM_{2.5}$ profile using the weather balloon procedure in the parking lot adjacent to PSI	23
Figure 15: Diurnal variations in traffic volume and speed northbound and southbound on I-93 on 11/18/2011.	24
Figure 16: PNC, $PM_{2.5}$, temperature, and relative humidity profiles during morning rush hour on 3/15/2012 at PSI.....	25
Figure 17: Wind roses showing the wind speed (left) and PNC (right) distributions that correspond with a particular wind direction from 1/21/12 to 2/9/12.	29
Figure 18: Average diurnal variation in PNC at PSI from 1/21/12 to 2/8/12 and traffic volume on I-93 on 2/3/12.....	30
Figure 19: Average $PM_{2.5}$ and PNC vertical profiles at PSI from 11/18/11 to 3/15/12.....	31

LIST OF TABLES

Table 1: Instruments used for data collection in this study.....	13
Table 2: Goodness-of-fit metrics for the CPC precision tests.....	16
Table 3: Summary Table of Vertical Profile Results.....	27

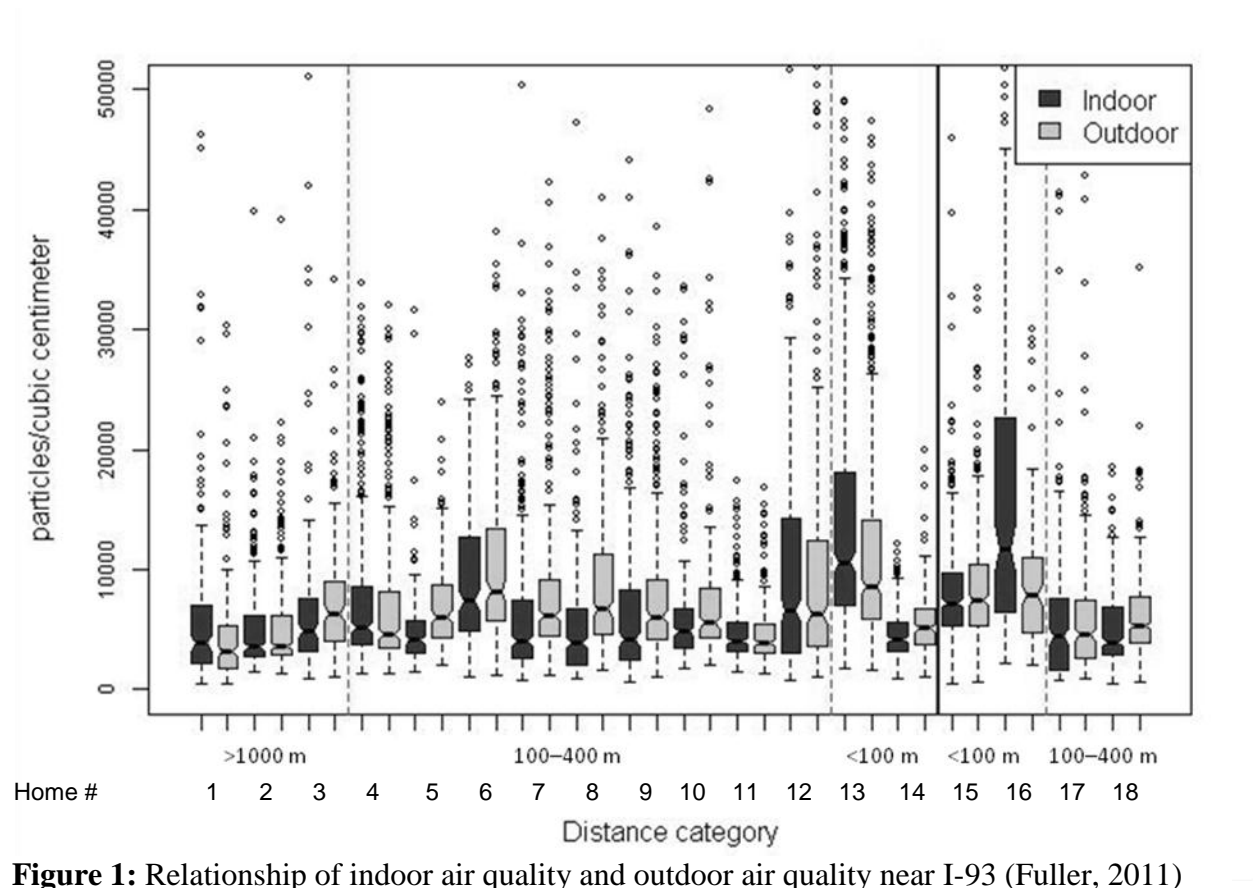
1.0 INTRODUCTION

1.1 Background

Many epidemiological studies have linked increased particulate matter (PM) exposure with adverse health effects (Oberdörster, 2005; Kreyling et al., 2002). Elevated exposures increase the prevalence of respiratory, cardiovascular, and neurological diseases (Oberdörster, 2005). In urban environments, the vast majority of particles are generated by industrial combustion processes and automotive sources in particular. Compared to PM in rural settings, PM in urban setting is primarily anthropogenic and more toxic due to both the size distribution and the composition of the PM (Kreyling et al., 2002). Because of the mechanisms by which it is made, anthropogenic PM tends to have a greater percentage of smaller particles, particularly ultrafine particles (UFP) in the <100 nm range, which can translocate in the body more efficiently (Oberdörster, 2005). In addition, this PM contains chemicals that the body is not typically exposed and adapted to.

The majority of combustion-generated particles in an urban region can be traced back to relatively few line and point sources in the area. The point sources include smokestacks related to industrial processes and power generation, and the line sources are major road ways. While there has been significant regulation on stack emissions resulting in 99% or greater reductions in PM emissions using control technologies, tailpipe exhaust has been controlled for particulates to a lesser degree (EPA, 1990). An analysis of the transport of particles generated on major roadways is necessary to understand the impact of these roadways on the local air quality. Several studies have looked at the pollutant distance-decay gradients perpendicular to major roadways at ground-level (Zhu et al., 2002; Zwack et al., 2011). Less attention has been directed towards the vertical gradients. In urban environments, this consideration is especially important

as people may live or work well above ground-level. The exposure above ground-level is largely to indoor air; however, building ventilation systems, depending on how they are operated, can cause the indoor air quality to be affected by and comparable to the outdoor air quality (Figure 1).



1.2 Previous Vertical Profile Studies

Vertical profiles of PM have been collected in several other studies. Morawska et al., 1999, measured the particle distribution on every 5th floor of two buildings in Queensland, Australia. They discovered that the particle number concentrations (PNC) were close in magnitude for particles >100 nm. UFP tended to decrease with height except for the first 5 floors where the particle counts were relatively similar.

Zhu and Hinds, 2004, collected carbon monoxide (CO) and PNC profiles near I-405 in Los Angeles, California. They developed an analytical model to predict the horizontal concentration gradient of PNC based on vertical profile measurements. The vertical profiles were collected using a scissor lift that could extend 18 m above ground-level. PNC decreased by approximately 50% over the 18 m vertical profiles with the maximum concentration occurring at 3 m.

Wu et al., 2002, also collected vertical profiles of PM_{10} , $PM_{2.5}$, and PM_1 along major roads in Macao, China. All three PM ranges decreased significantly with height, with the majority of the decrease occurring within the first 10 m of elevation. $PM_{2.5}$ was found to decrease by 40% over the 79 m profile. The trend was more significant for the larger particles, such that the PM_1 profile was the most uniform. The profiles collected in the morning were not significantly different than those collected in the afternoon. Wu et al. attributed the PM_{10} profiles to road dust and the $PM_{2.5}$ and PM_1 to tailpipe exhaust.

McKendry et al., 2004, was able to obtain profiles for PM_{10} and $PM_{2.5}$ as well as for temperature, wind direction and speed, and relative humidity up to 375 m using a weather balloon setup. Their objective was to establish the effect of domestic wood and coal burning in Christchurch, New Zealand, on particulate levels. PM_{10} and $PM_{2.5}$ decreased significantly for the first 40 m and then remained relatively constant. The high concentrations at ground level were attributed to a ground-based temperature inversion, which trapped the PM near the ground, and the high source emissions from domestic fires. However, the $PM_{2.5}$ profile was uniform on a day without domestic burning, suggesting the source strength had the greatest influence on the vertical $PM_{2.5}$ concentration gradient.

1.3 Objectives

The objective of the research presented here is to provide an assessment of the vertical profiles of PM near Interstate 93 (I-93) with respect to meteorological conditions. Trends in PNC and particle mass concentrations with height are analyzed to characterize the impact of temperature, wind direction, and traffic conditions on both the magnitude and the slope of the PM profiles.

This objective addresses a data gap in the literature and in the Community Assessment for Freeway Exposure and Health (CAFEH). The goal of the CAFEH study is to characterize the exposure associated with highway pollution and the related health effects. The study has collected extensive ground-level air contaminant data in four near-highway neighborhoods in Boston. The research presented in this report provides an understanding of the vertical profiles in one of the CAFEH study areas. In addition, the PNC and PM_{2.5} profiles combine a fine spatial resolution with a large sampling height, which is unique for near-highway vertical dispersion studies.

2.0 THEORY

2.1 Buoyancy

Vertical transport, which governs the vertical concentration gradient, is comprised of buoyancy and turbulent motion. Buoyancy is caused by differential heating that leads to temperature gradients, which in turn causes air flow. The principle of buoyancy is the same for all fluids, gases and liquids alike: less dense medium float above more dense ones. When comparing two different parcels of air, warmer ones will rise above cooler ones according to the ideal gas law:

$$(1) \rho = \frac{P * MW_{air}}{RT}$$

where ρ is density, P is pressure, MW_{air} is the molecular weight of air, R is the ideal gas constant, and T is the temperature (Jacob, 1999). Increasing the temperature decreases the density; therefore, hotter air is less dense than colder air and will rise above it.

When considering a particular parcel of air, its vertical motion due to buoyancy is dependent on its temperature relative to the air around it. If the parcel of air behaves adiabatically (i.e., it does not exchange heat with the surrounding air), its motion up or down will cause it to change temperature. This temperature gradient is referred to as the adiabatic lapse rate (Γ):

$$(2) \Gamma = -9.8K/km$$

The atmospheric lapse rate and the adiabatic lapse rate can be compared to determine the stability of the atmosphere (Figure 2). When the atmospheric lapse rate is less steep and more negative than Γ (i.e., it cools more than 9.8K/km), the parcel of air will continue to rise if it is displaced upwards and will continue to sink if it is displaced downwards. This scenario is referred to as unstable air, which leads to the atmosphere being well mixed. When the atmospheric lapse rate is greater than Γ , the parcel of air will return to its original position if it

risers or sinks. This condition is called a stable lapse condition because little mixing occurs.

Lastly, if the atmospheric lapse rate is the same as Γ , buoyancy does not impact the vertical transport and turbulence acts as the primary transport mechanism.

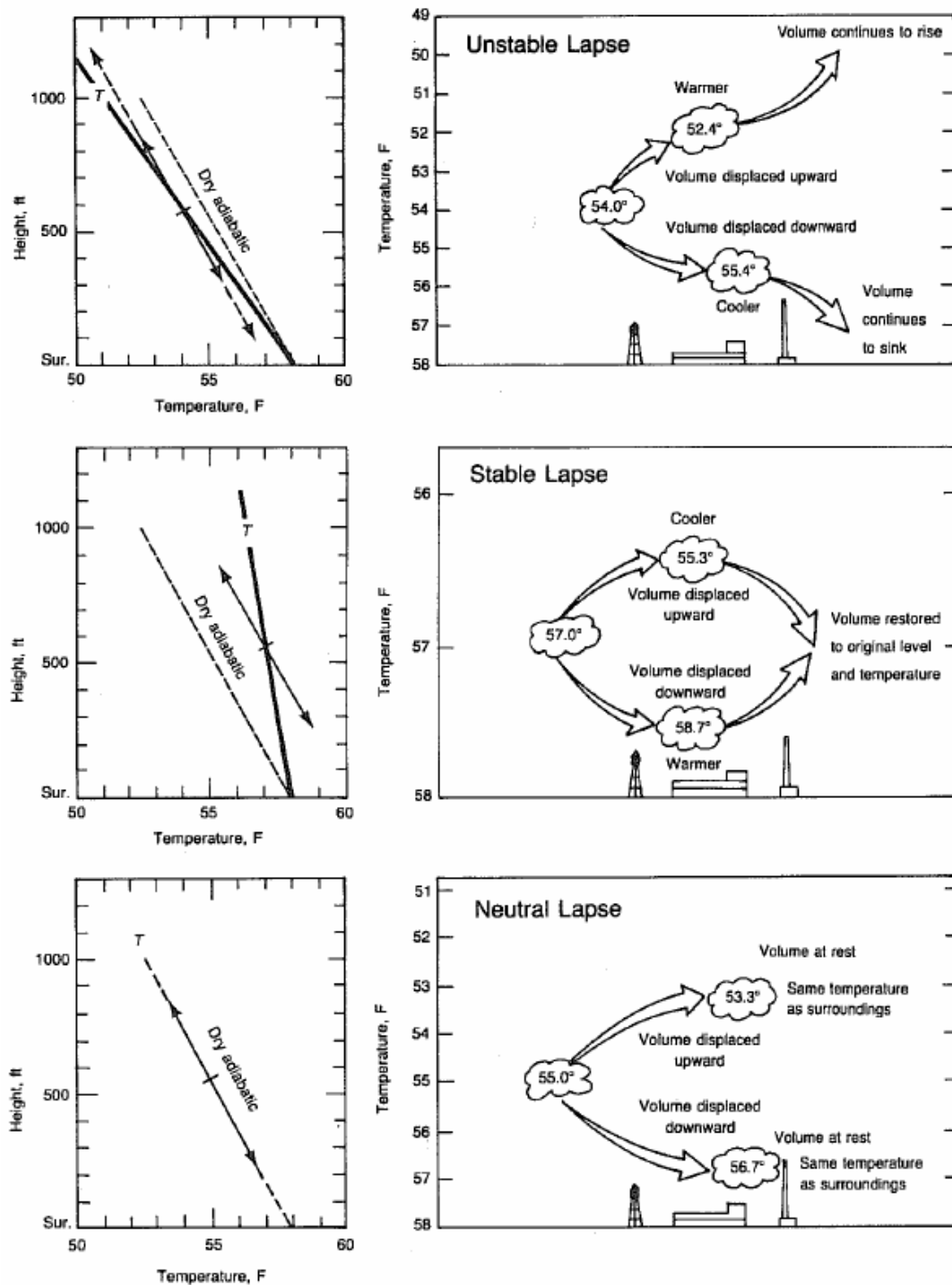


Figure 2: The effect of the actual lapse rate on vertical stability (Cooper and Alley, 2011)

As indicated in Figure 3, certain diurnal trends in atmospheric stability emerge due to differential heating. Before dawn the earth radiates heat from the surface into the air, cooling the earth to a lower temperature than the air above it. This stable condition causes a ground-based inversion where the air is stratified even close to ground-level. Once the sun rises, the earth warms faster than the air. Over the course of the day the atmospheric lapse rate shifts until it is more negative than Γ , leading to increased mixing up to the mixing height, denoted z_i in Figure 3. The mixing height is the altitude at which the superadiabatic lapse rate (the dashed line) connects with the subadiabatic lapse rate remaining from the night surface cooling (the thin solid line). The mixing height gets larger later in the afternoon as the air is heated at higher altitudes. At dusk, the surface again starts cooling down faster than the air, starting the cycle over again (Figure 3).

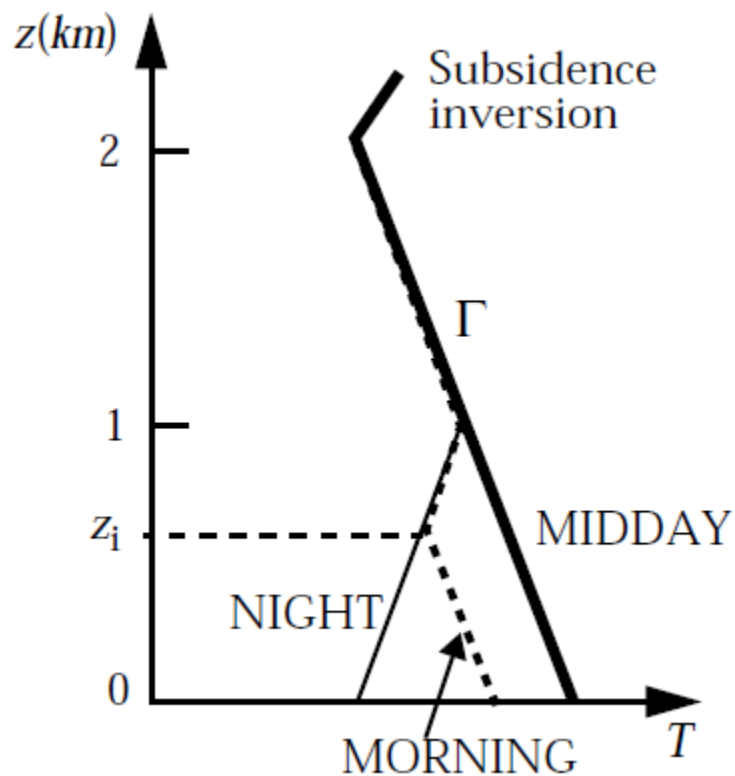


Figure 3: Typical diurnal variation of temperatures near the ground (Jacob, 1999)

2.2 Turbulence

Buoyancy dictates the air flow in the vertical direction. In unstable conditions, the vertical transport both up and down is accelerated. The two-way flow of air due to buoyancy leads to irregularity in the flow field, which is called turbulence. The turbulent flux can be predicted using an empirical expression similar to Fick's law for molecular diffusion:

$$(3) \bar{F} = -n_a K_z \frac{\partial \bar{C}}{\partial z}$$

where \bar{F} is the turbulent flux, n_a is the number density of air, K_z is the turbulent diffusion coefficient, and $\frac{\partial \bar{C}}{\partial z}$ is the time-averaged vertical concentration gradient. The flux depends linearly on the time-averaged concentration gradient.

Turbulence leads to a more uniform concentration gradient over time. Consider a plane separating clean air above from dirty air below. Buoyancy will cause increased flow through the plane in both directions. Clean air from above the plane will dilute the dirty air below while dirty air pollutes the clean air above. When this system reaches equilibrium, the concentration above and below the plane will be the same even though the net transport of air equals zero.

2.3 Particle Measurements

Two different types of measurements are used to express the PM concentration. PNC is the number of particles contained within a certain volume of air. Because of the abundance of UFP compared to larger particles, PNC is dominated by small particles. When considering UFP in particular, they are more influenced by turbulence than gravitational settling due to their small size. Therefore, they will follow the flow of air rather than settle out. As a result, PNC is more susceptible to buoyancy.

PM_{2.5} is a particle mass concentration of all the particles smaller than 2.5 μm in diameter. The Environmental Protection Agency (EPA) regulates PM_{2.5} as a criteria pollutant. The primary

standards are a $15 \mu\text{g}/\text{m}^3$ annual average and a $65 \mu\text{g}/\text{m}^3$ 24 hour average. Larger particles account for a greater percent of the $\text{PM}_{2.5}$ concentration due to their greater mass despite being outnumbered by smaller particles (Figure 4). These large particles are influenced by settling more than buoyancy, which results in the $\text{PM}_{2.5}$ concentration being only loosely correlated with atmospheric stability.

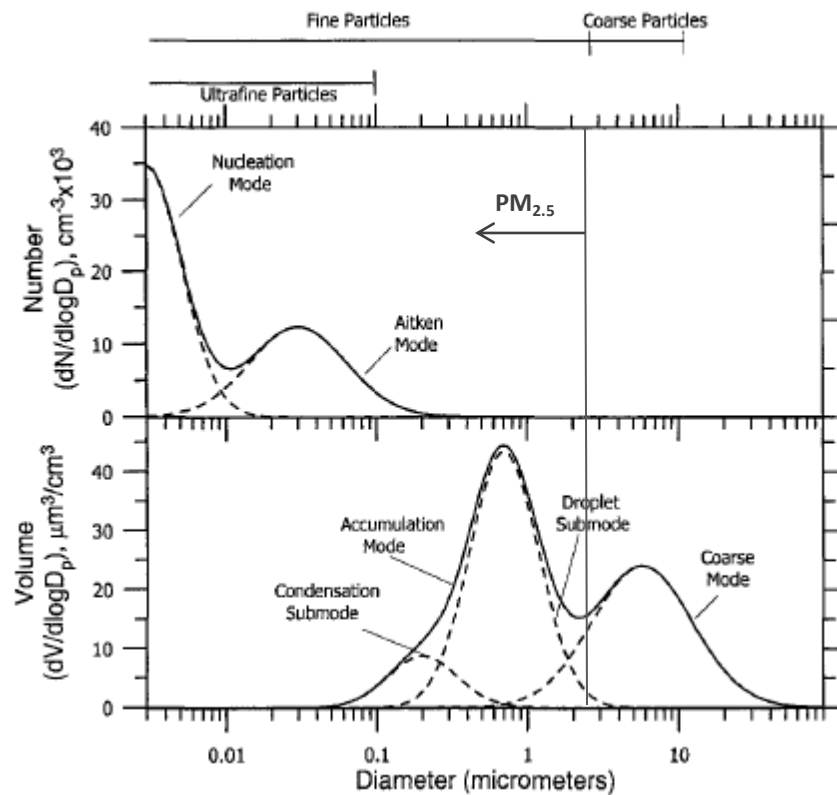


Figure 4: Typical number and volume distributions of atmospheric particles. Assuming density is constant for each diameter particle, the mass distribution will be a scalar of the volume distribution (Seinfeld and Pandis, 2007)

3.0 METHODS

3.1 Site Description

All monitoring for this project took place at the Pine Street Inn (PSI) in the South End of Boston. PSI is located 100 m west of I-93 and 400 m south of the Mass Pike (I-90) (Figure 5). I-93 is a seven lane highway as it passes PSI that runs north to south through Boston. Approximately 170,000 vehicles use the highway per day where it passes PSI, divided into three lanes southbound, which were heavily congested during the hours looked at in this study, and four lanes northbound. I-90 runs east to west with traffic volumes of approximately 130,000 vehicles per day.



Figure 5: Site Locus

The PSI was selected as the monitoring site because of its proximity to both highways and because of the 11-story tower connected to the main building. The tower, which faces east towards I-93, was historically a fire tower but currently is unused by PSI. The first seven stories house a staircase, while the last four are accessible by ladders. The ladders and hatches between

the final stories of the tower prevent transporting any bulky equipment past the seventh floor (Appendix A). Floors 9–11 are outside the tower; the ninth floor has crenellations that extend out from the tower (Figure 7). The roof of the building, which was accessible from the seventh floor of the tower, was used to take wind measurements and held the stationary monitoring box discussing in Section 5.3. The roof of the building was above the urban canopy so the wind speed and direction were not affected by the surrounding buildings.

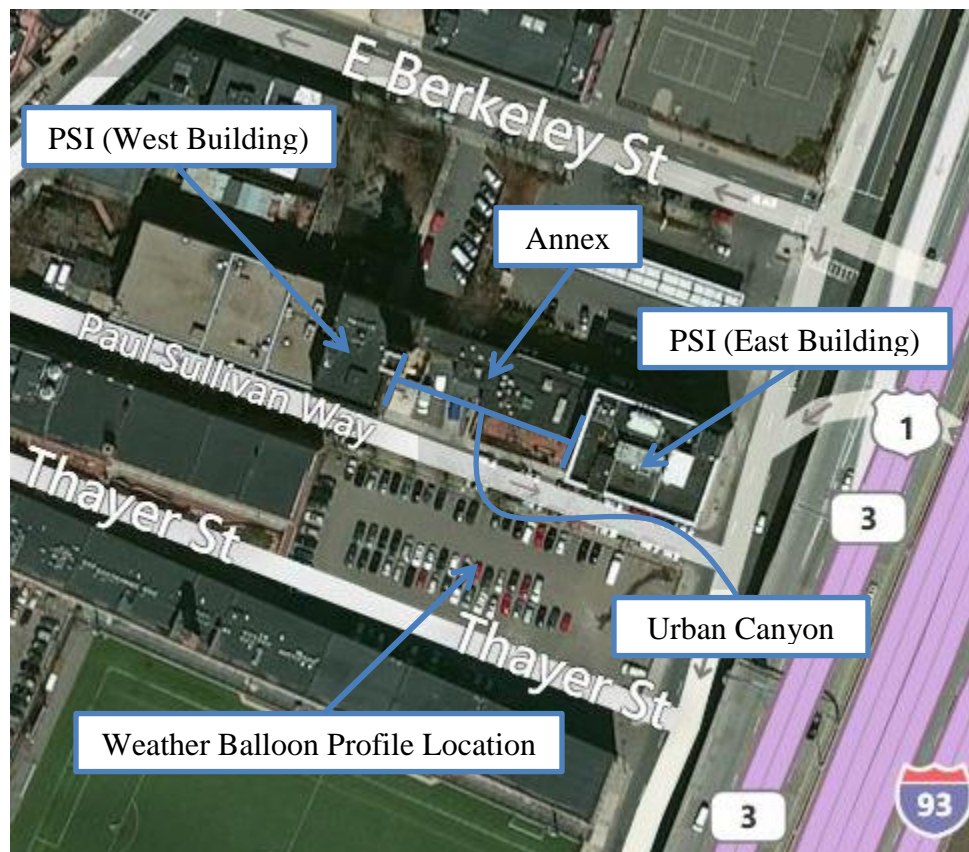


Figure 6: Aerial view of PSI

The local urban canopy impacts the wind patterns in the vicinity of the tower. The urban canopy is the atmospheric layer below the mean building height in a city. This layer is dominated by the microscale meteorological conditions that arise from the complex structural layout of the layer. Although the last five stories of the tower extend above the urban canopy, the first six stories will be affected by the buildings near the tower. PSI consists of two buildings, each 24 m

tall and connected from east to west by a 10 m tall annex (Figure 7). The tower is located on the eastern side of the western building. These buildings result in an urban canyon with winds prevailing from south to north through the canyon. The vertical profiles, collected on the eastern face of the tower, are on the western edge of this canyon. In addition, I-93 is raised 12 m where it passes the PSI, altering the emission height of that line source.

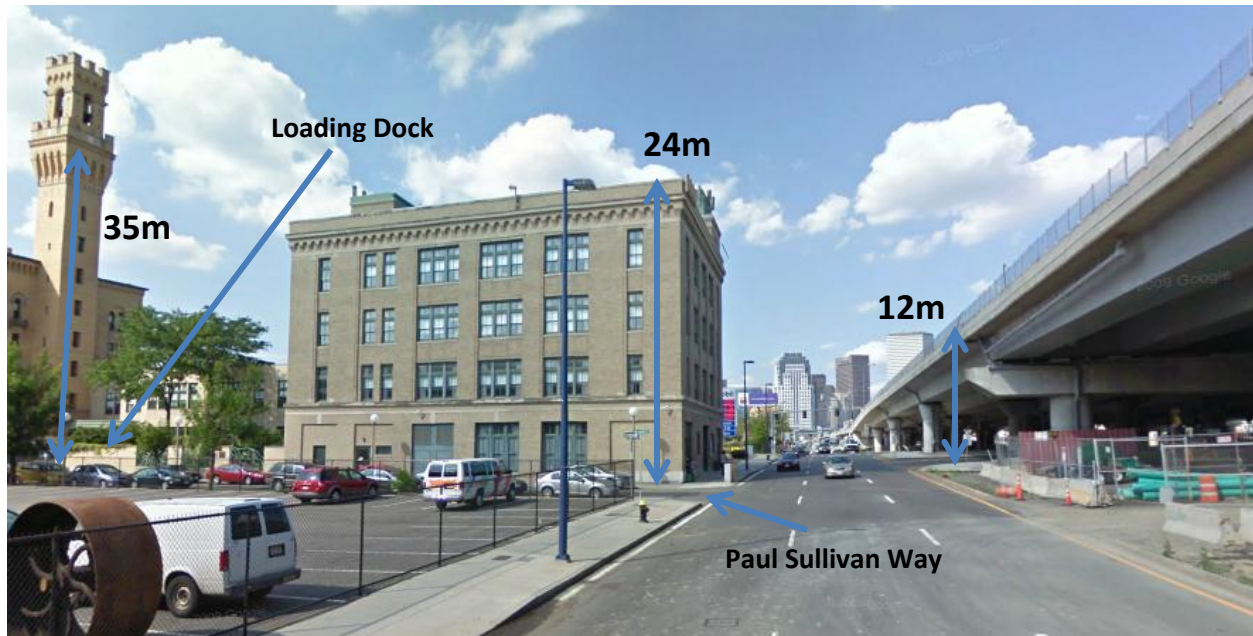


Figure 7: Street-view of I-93 and PSI with relevant structure heights looking north

3.2 Experiment Procedure

3.2.1 Pulley System

The vertical profiles were collected using a pulley system that hoisted the instruments in a customized pelican case up the side of the tower. The pelican case was hooked on to a rope which was fed through the pulley at the top of the tower and back down to a winch at ground level. The pulley was secured to the crenellations on the ninth floor and hung down one meter to get over the lip at the base of the crenellations (Appendix B). The profiles thus ended one meter below the pulley, the final profile height was 35 m above the street. The battery-powered winch lifted the pelican case by spooling the rope. The rotational velocity of the winch depended on the

weight of the case, which remained relatively constant for each profile (the weight increased slightly with height as more of the extension cord was lifted off the ground). The instantaneous height of each profile was determined based on the start and end time of the profile, which took approximately five minutes, assuming a constant velocity of the pelican case. These instantaneous heights were used to average the data into meter-sized bins. Finally, the profile collected on the way up was averaged with the profile collected on the way back down, resulting in one 10-minutes profile with a resolution of 1 m.

Table 1: Instruments used for data collection in this study

Instrument	Model	Output	Logging Interval (s)
Pelican Case			
Condensation Particle Counter	TSI 3781	6–3000nm Particle Count (#/cm ³ , +/- 10%)	1
SidePak Aerosol Monitor	TSI AM510	<2.5µm PM Concentration (mg/m ³)	10 (moving avg)
HOBO Temperature and Relative Humidity Probe	HOBO U12-011	Temperature (°C) and Relative Humidity (%)	1
Turbometer	271	Wind Speed and Direction	NA
Defender 500 Series	BIOS 510-H	Flow Rate (mL/min, +/- 1%)	NA
Stationary Monitor			
Condensation Particle Counter	TSI 3783	7-3000nm Particle Count (#/cm ³ , +/- 10%)	60 (moving avg)
Davis Instruments Vantage Vue Integrated Sensor Suite	Davis 6357	Temperature, Wind Speed, Wind Direction, Relative Humidity, and Precipitation	1800

The pelican case was equipped to hold a condensation particle counter, model 3781 (CPC-3781), a SidePak aerosol monitor, and a HOBO temperature and relative humidity probe (Table 1). The particle instruments received air from outside the box via three inches of conductive tubing. They received power from extension cords that ran out the window on the fourth floor of the tower and into the pelican case. The HOBO probe was clipped to the outside of the box. The turbometer is a handheld anemometer used to take a wind speed and direction

measurement on the roof of PSI during each profile; however, for the second half of the study (January to March), the stationary monitor located on the roof of the PSI was used for meteorological data instead.

3.2.2 Stationary Monitoring Box

The stationary monitoring box was located on the southwest corner of the roof at PSI, approximately 24m above ground-level. The box was equipped with an condensation particle counter, model 3783 (CPC-3783), and a Davis Instruments meteorological station (Table 1). The wind vane did not operate properly, so the wind direction and speed data was not used. The box was installed on 1/20/2012 and collected data until 3/15/2012, the last day of monitoring. The CPC-3783 only ran until 2/9/2012.

3.2.3 Weather Balloon

The weather balloon was used to get an extended temperature and $PM_{2.5}$ profile up to 70 m above ground. The profile was collected in the parking lot on the other side of Paul Sullivan Way (Figure 6). The weather balloon was tethered to the winch by a 90 m rope. Once inflated with helium, the SidePak and HOBO probe were attached to the weather balloon. Similar to the pulley system, ascending and descending profiles were collected. Each profile took ~20 minutes; every 30 seconds, an angle measurement was taken to determine how far the wind had pushed the balloon from vertical. The angle measurements were linearly interpolated for the data analysis. Assuming the winch operated at a constant rate, the height of the balloon at a given time could be calculated using the start and end times of each profile and the angle measurements.

3.3 Quality Assurance and Quality Control

Quality assurance was primarily implemented in the field through a series of steps listed in the experimental procedure (Appendix B). Before each monitoring session, all the instruments were synchronized to the same time. A zero filter was used to test the lower limit of the particle

instruments. In addition, the SidePak had a zero calibration that was conducted with the zero filter. The flow rate of the particle instruments was also measured in the field using the Defender 510-H before the first profile. Flow rates in the range of 1400–1600 mL/min for the SidePak and 500–700 mL/min for the CPC-3781 were required to proceed with monitoring. During each profile, observations were recorded in the field log. Any vehicle activity in the loading dock or along Paul Sullivan Way (Figure 7) was noted and addressed in Section 4.1.5. Once the monitoring session was concluded, the CPC was dried by draining the water in the CPC as specified in the CPC-3781 manual and stored until the next session. During data processing, data flagged with instrument errors were discarded.

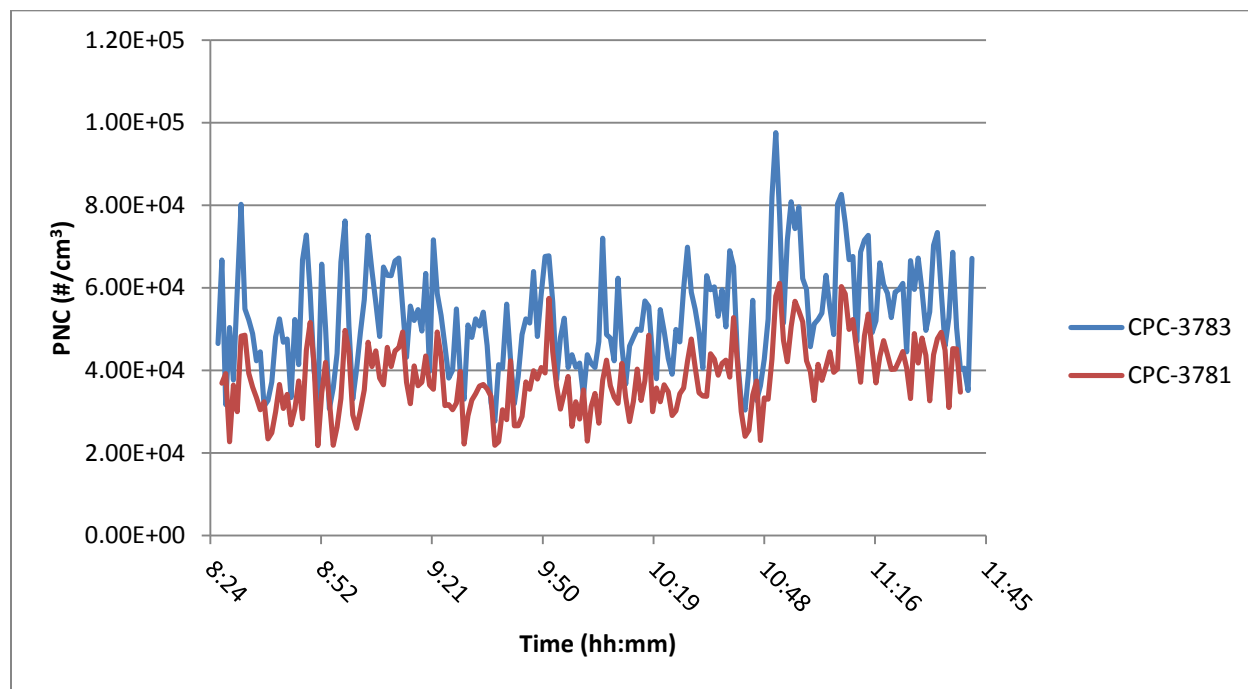


Figure 8: CPC comparison test in the stationary monitoring box at PSI on 3/15/2012

3.3.1 Condensation Particle Counter

Several quality control experiments were conducted to ensure the precision and accuracy of the instruments used in this study. The particle instruments were exposed to a spike to determine the response times of the instruments. For both the CPC and the SidePak the response times were

less than one second and thus time corrections were not implemented in the data processing. The WCPC and the EPC were compared in the field at PSI and in a laboratory setting as a test of precision (Figure 8 and 9). The CPC-3783 and CPC-3781 obtain similar particle counts at low concentration in the lab; however, in the field when exposed to concentrations an order of magnitude larger the CPC-3781 underestimates the particle count relative to the CPC-3783 by 28.5% (Table 2). The R^2 of both tests were high indicating that the residuals were homoscedastic and that the particle counts of each instrument were linearly correlated. Both instruments generally agree on the relative increase or decrease in PNC, but the magnitude of the concentration may be off by 29% at high concentration. The Nash-Sutcliffe Efficiency Criterion (E) is the most resilient goodness-of-fit metric as it accounts for both bias and variance. A value of 1 indicates perfect agreement between the datasets.

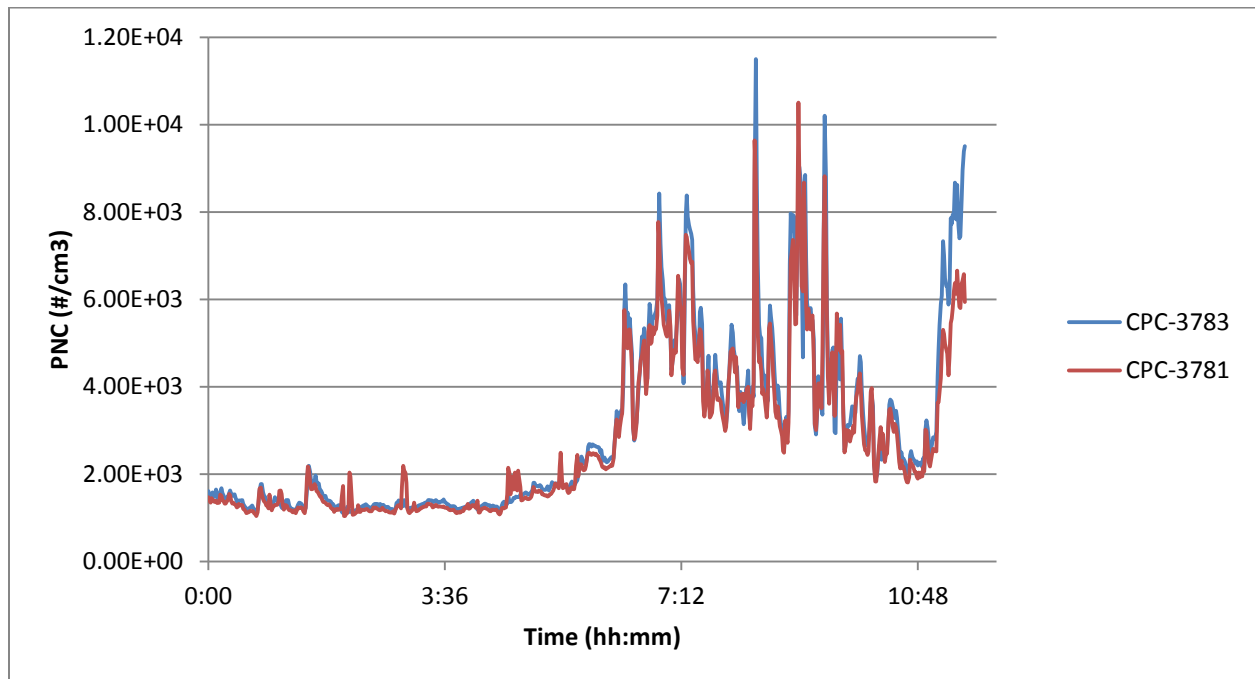


Figure 9: CPC precision test in the laboratory at Tufts University on 4/5/2012

Table 2: Goodness-of-fit metrics for the field and laboratory precision test of the CPC-3781 and the CPC-3783. The unbiased metrics were calculated by raising the CPC-3781 concentrations 28.53%.

Location		Bias (%)	E (Nash-Sutcliffe)	R ²
PSI	Biased	28.53	-0.67	0.82
	Unbiased	0.00	0.75	0.82
Laboratory	Biased	6.67	0.93	0.95

3.3.2 SidePak Aerosol Monitor

The SidePak AM510 aerosol monitor measures the light scattering of particulates as they pass through an impactor assembly to determine the mass concentration of the particles. Compared to Federal Reference Method (FRM) PM_{2.5} samplers, the SidePak shows a slight bias (root mean square error of 4.31 µg/m³). Over a long sampling time, the SidePak is strongly correlated with the FRM sampler.

4.0 RESULTS AND DISCUSSION

4.1 Vertical Profile Gradient

4.1.1 Temperature

The relationship between the temperature profile and the adiabatic lapse rate determines which direction a parcel of air will travel. To distinguish between whether the parcel of air will rise or fall, the temperature profiles have been adjusted such that the adiabatic lapse rate is a vertical line (Figure 10). Profiles with a positive slope after this adjustment are considered stable, those with a negative slope unstable, and those that are vertical neutral. This adjustment amounts to a 0.35°C change at the top of the profile, 0°C at the bottom, and a proportional amount for the points in between.

The diurnal variation in temperature shown in Figure 3 is also apparent in the profiles from 12/16/11 and 12/9/11. The temperature profile shifts from a positive slope in the morning to a negative slope in the afternoon (Figure 11). The temperature was too low on 11/18/11 to reflect the complete diurnal cycle.

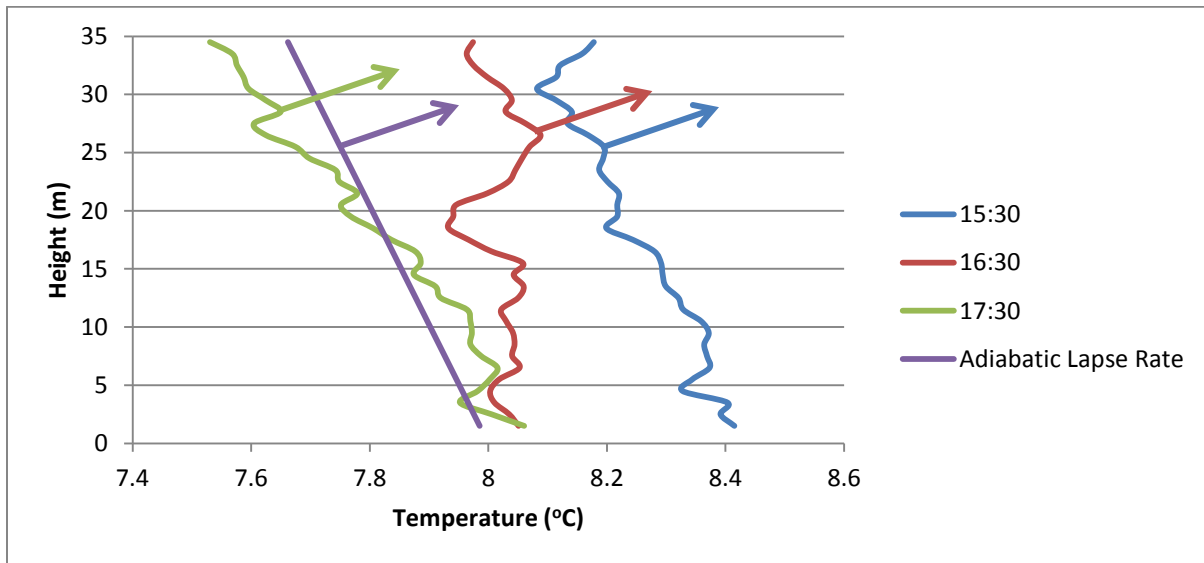


Figure 10: Vertical temperature profiles in the afternoon at PSI on 11/18/2011. The arrow indicates the adjustment of the temperature profiles.

4.1.2 Particle Number Concentration

After this adjustment, two types of atmospheric conditions emerge: 1) the temperature profile is close to neutral, and 2) the temperature decreases significantly with altitude. The first scenario includes all the profiles where the temperature profile remains within a degree of the surface temperature. In this scenario, the temperature profiles and the PNC profiles have the same slope (Figure 11). When the temperature profile is unstable, the particles will tend to continue rising above 35m if they are displaced upwards or continue to sink if they are displaced downwards. This mechanism causes the particle count to increase close to the ground and decrease higher up as the particles are mixed above 35m. Conversely, when the temperature profile is slightly positive the particles will resist turbulent motion and stay in their original position. Therefore, pollution is trapped once it is emitted until the atmosphere become unstable and dilutes the polluted air with clean air from above.

Furthermore, in this scenario the atmospheric lapse rate is close to the adiabatic lapse rate, making the effect of measurements errors more pronounced. A small deviation in the temperature could result in a change in the atmospheric stability from stable to unstable, which would impact PNC significantly.

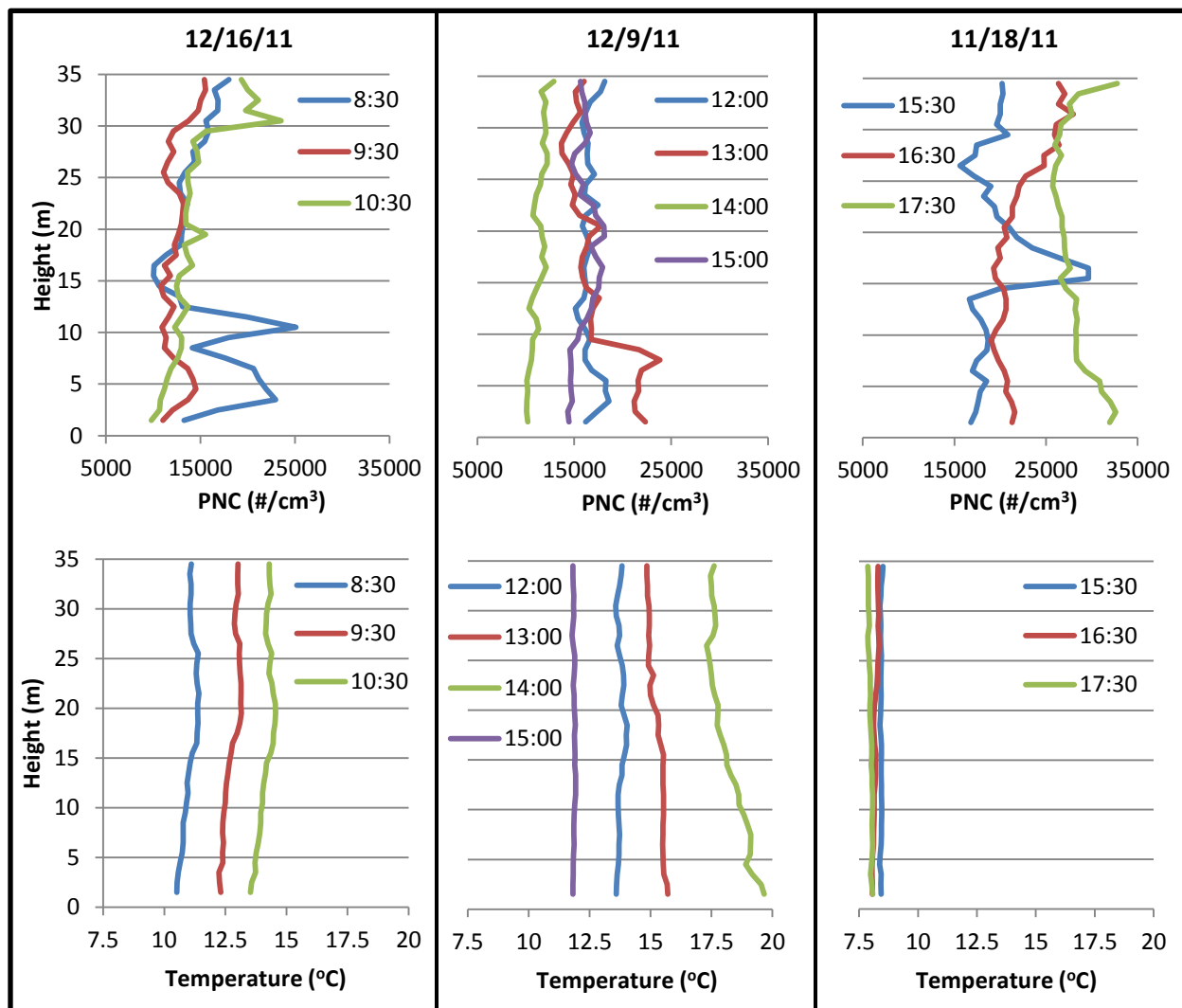


Figure 11: Vertical Profiles of PNC and temperature at PSI from 11/18/11 to 12/16/11. The temperature profiles are corrected for the adiabatic lapse rate.

The second scenario when the temperature drop significantly with height is indicative of highly unstable atmospheric conditions. In this scenario, the rapid vertical transport due to buoyancy results in the atmosphere being well mixed until it reaches an inversion, which occurs at a higher altitude than obtained in these profiles. Therefore, the particle count will remain constant. The magnitude of the particle count in this scenario will depend on the source strength and the mixing height, which is the height of the inversion. A higher mixing height has a greater volume of air in the mixed layer, which lowers the particulate concentrations.

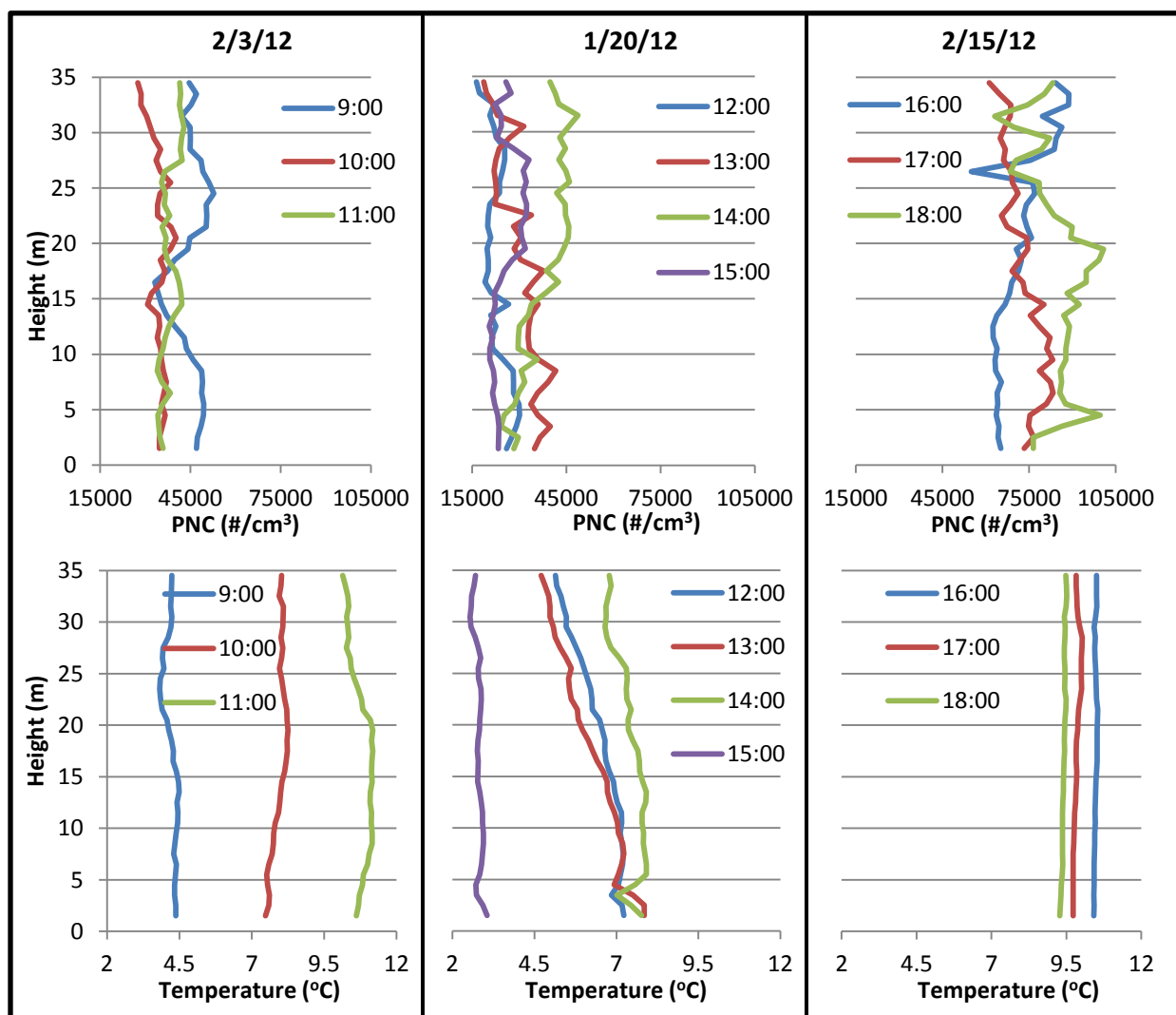


Figure 12: Vertical Profiles in PNC and temperature at PSI from 1/20/12 to 2/15/12. The temperature profiles are corrected for the adiabatic lapse rate.

4.1.3 Particle Mass Concentration

The $PM_{2.5}$ concentration is uniform over the profile height. Since $PM_{2.5}$ is not affected by buoyancy on a short timescale, turbulent motion becomes the predominant transport mechanism, which causes the concentration gradient to be relatively uniform, indicating mixed conditions. In addition, the $PM_{2.5}$ concentrations do not vary on an hourly timescale (Figure 13).

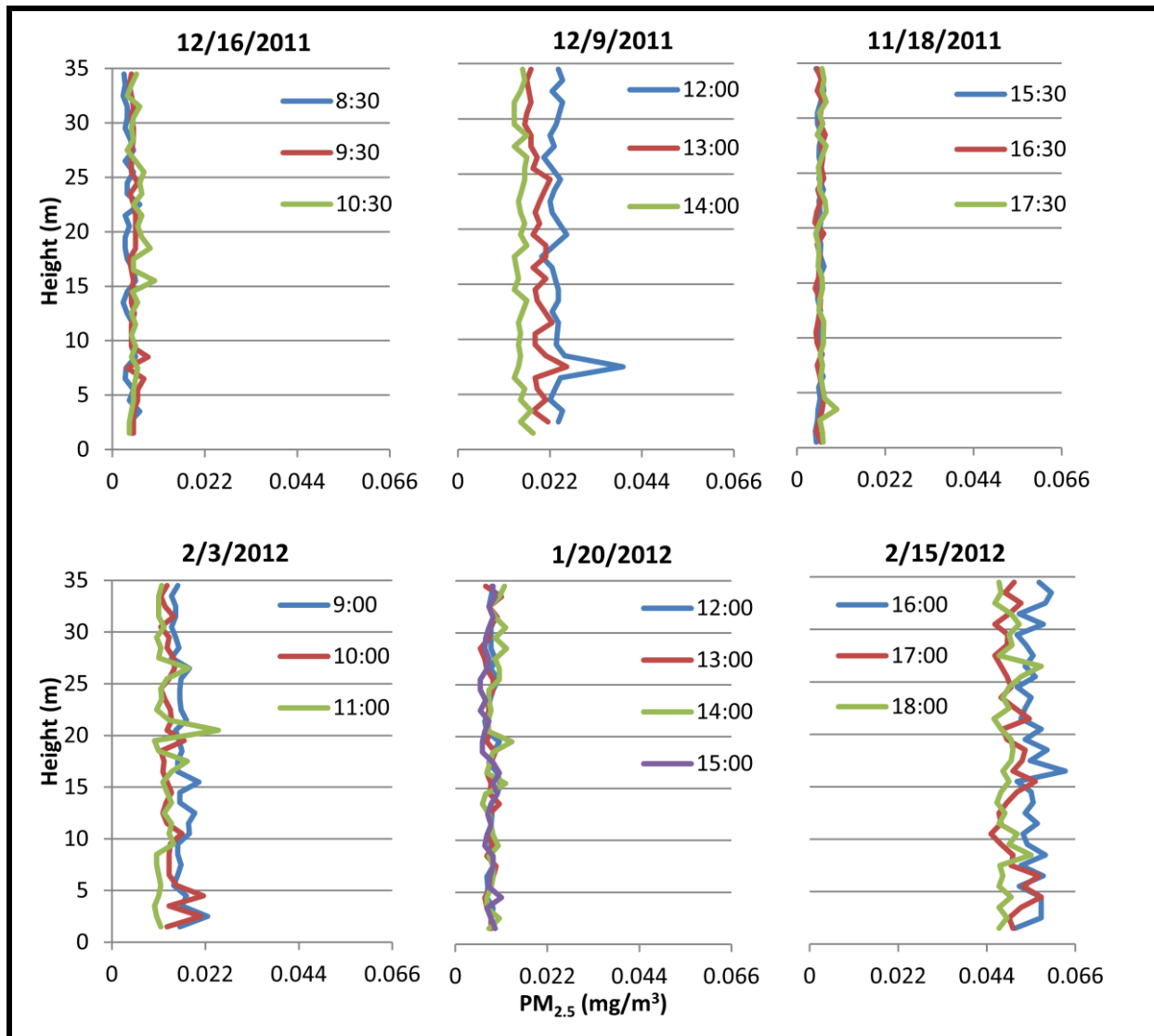


Figure 13: Diurnal variations in $PM_{2.5}$ with respect to height at PSI from 11/18/11 to 2/15/12.

The $PM_{2.5}$ concentration does decrease in the extended profile on the way up at an elevation of 25 m (Figure 14). This is the approximate scale height of the urban canopy since most the buildings in the vicinity are 25 m tall. At the peak of the profile it returns to the ground-level concentration and remains there for the down profile. The decrease in $PM_{2.5}$ is a result of the changing position of the weather balloon due to wind shifts, which affects where the balloon is located in the sky and therefore what air it is monitoring.

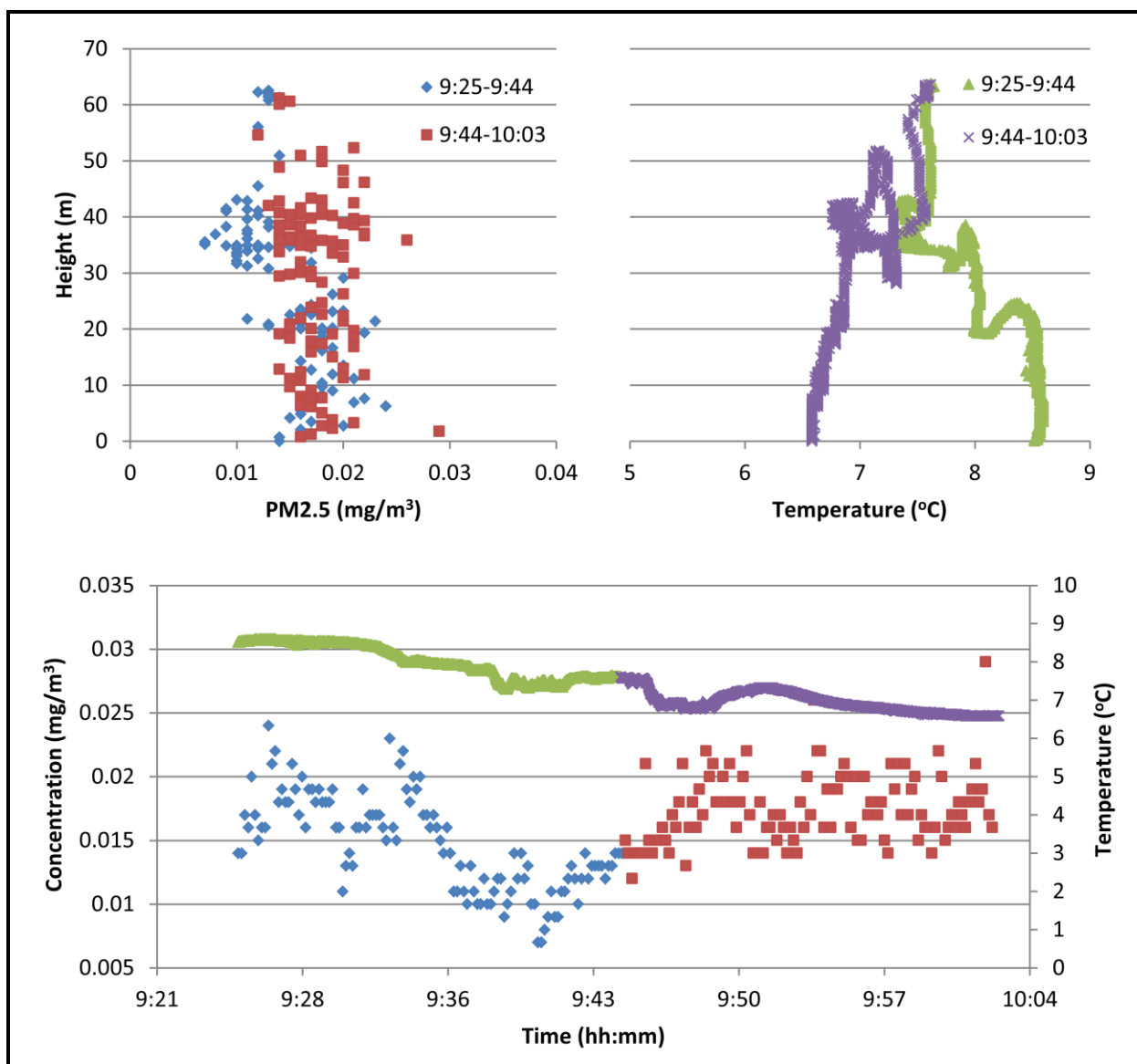


Figure 14: Extended $PM_{2.5}$ profile using the weather balloon procedure in the parking lot adjacent to PSI

4.2 Vertical Profile Magnitude

4.2.1 Wind Direction and Source Strength

The wind direction strongly influenced PNC and $PM_{2.5}$ concentrations at PSI since the source of the particles depended on the wind direction. When the wind is from the west, PSI receives urban background pollution from Boston. When it is from the north and east, the highways and sources to the east impact the particle concentrations. For the days included in Figures 11 and 12, the

wind ranged from the southwest to northwest with the exception of 2/3/12, when it came from the north off I-90, and 2/15/12, when it came from the east off I-93 (Table 3). An additional day of monitoring was conducted on 3/15/12 to capture the early morning rush hour when the wind was blowing from the east with PSI downwind of I-93 (Figure 16). All three of the days with north or east winds had elevated PNC and PM_{2.5} concentrations compared to days with west winds.

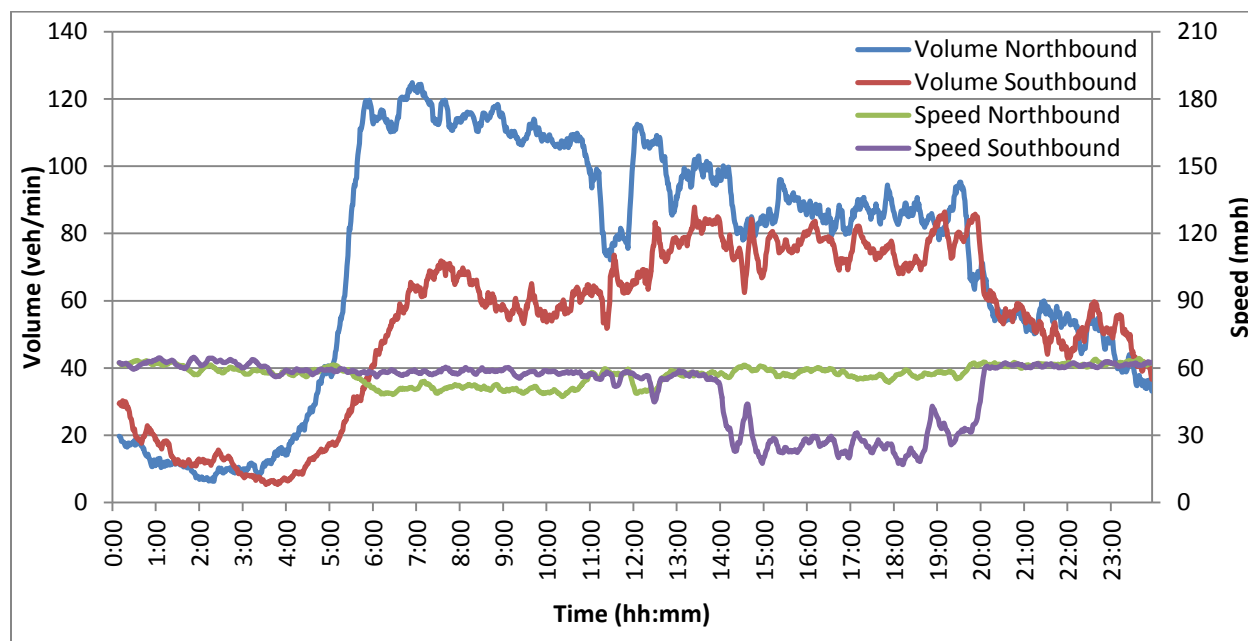


Figure 15: Diurnal variations in traffic volume and speed northbound and southbound on I-93 on 11/18/2011

The increase in PNC is attributable to automobile emissions on the highway. The proximity of the highway allows particles generated on the highway to reach PSI before they have coagulated and condensed into larger particles, which would lower the particle count. PNC has a relatively short lifetime in the atmosphere due to coagulation, condensation, and reaction, so proximity to the source is an important factor.

Automobile emissions are a small source of $PM_{2.5}$ compared to other industrial and commercial sources. The largest $PM_{2.5}$ source to the east of PSI is Logan airport, which accounts for 1% of mobile $PM_{2.5}$ emissions in the greater Boston area (Ratliff, 2009). This percentage is high considering the small area of the airport relative to the size of Boston. The airport acts as a large area source, which will emit a wide plume towards Boston during east winds.

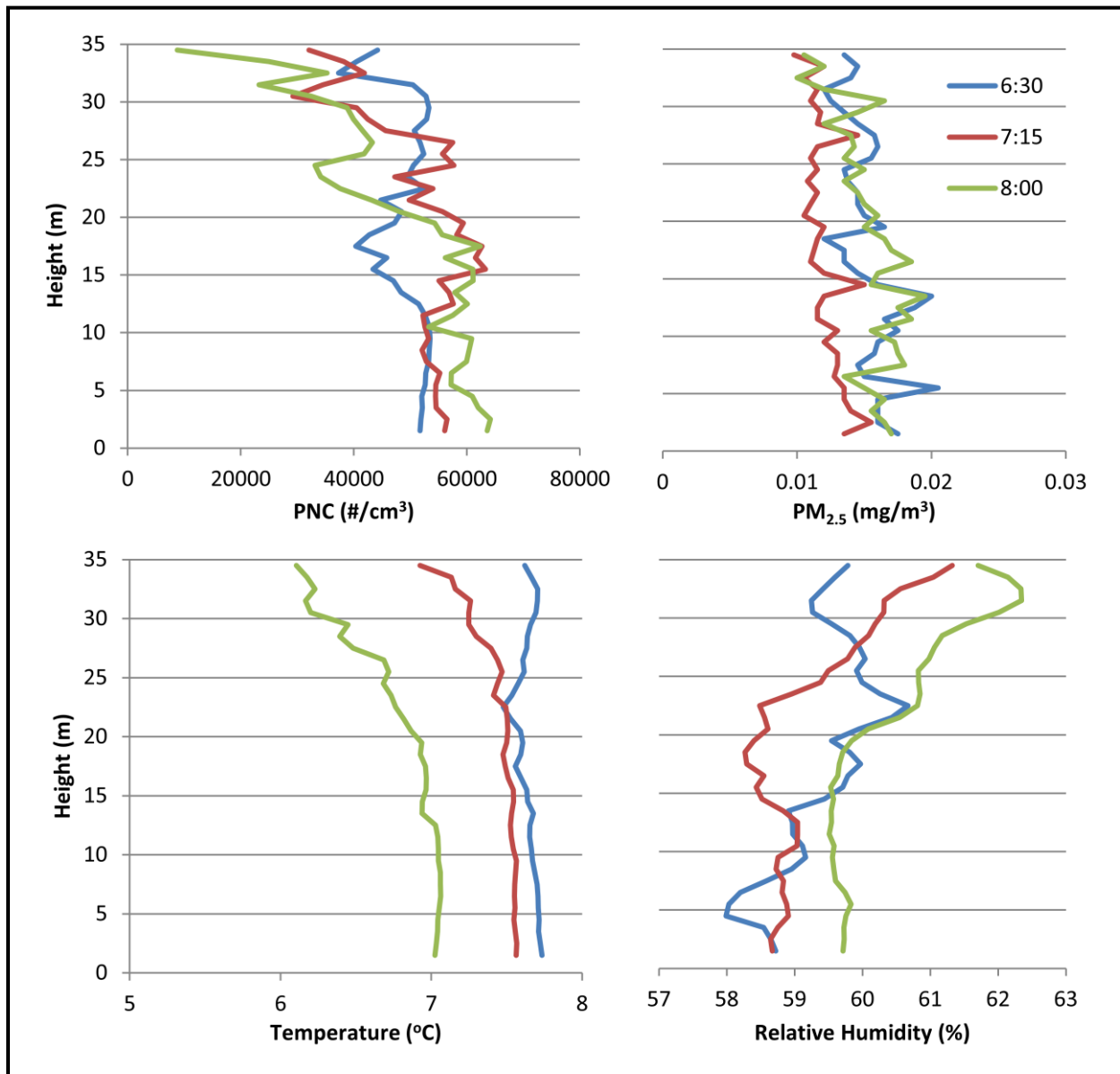


Figure 16: PNC, $PM_{2.5}$, temperature, and relative humidity profiles during morning rush hour on 3/15/2012 at PSI.

4.2.2 Atmospheric Stability

The magnitude of the PNC profiles also depends on the variation in the temperature profiles over the course of the day. Despite moderate traffic reductions after the morning rush hour, the PNC concentration increased from morning to midday on 12/16/11 and 12/9/11 (Figure 15). The superadiabatic and neutral temperature profiles suggest that on these days the particulate matter is trapped as new emissions during this period add to the particulate levels (Figure 11). The levels will increase until a subadiabatic condition occurs, such as when the sun heats up the ground faster than the air above it, allowing a greater degree of vertical mixing. In the winter, the atmospheric lapse rate does not become subadiabatic until around 14:00. The end result is increased mixing occurs around 14:00, and then the air is repolluted during the afternoon rush hour (Figures 11 and 12). $PM_{2.5}$, on the other hand, does not vary on an hourly timescale, so diurnal variations in atmospheric stability do not affect its magnitude.

The profiles from 3/15/12 also demonstrate the impact of atmospheric stability on PNC. The temperature profiles indicate the neutral conditions on 3/15/12 up to 20–25 m elevation giving way to unstable conditions higher up, especially in the 07:15 and 08:00 profiles. As a result, PNC above 20 m drops off as it is able to mix upwards, while below 20 m the PNC is elevated. The concentrations below 20 m are not as high as on 2/15/2012 because some of the particles are transported to the unstable region due to turbulence. In comparison, the temperature profiles from 2/15/2012 range from neutral (16:00) to slightly stable (17:00 and 18:00), causing the particles to remain trapped near the ground and the concentrations to rise. The concentrations exceed those from 3/15/2012 despite the traffic conditions being worse on that day, suggesting that atmospheric stability has a greater effect on the PNC concentration than source strength.

4.3 Additional Variables

Several variables outside the scope of this study affected specific days or profiles and need to be addressed. Temporal factors influenced the profiles, even though the profile collecting process took only 10–15 minutes. Local, pulse sources, such as trucks using the loading dock, could increase the PNC near ground-level. Emissions from before a profile was collected could also rise and cause a high concentration zone at a specific elevation. By analyzing the up and down profiles separately and using observations from the field, some of the uncharacteristic spikes in the PNC profiles were explained. For example, the spikes at 13:00 on 12/9/11 and at 15:30 on 11/18/11 both arose from a source being introduced in between the up and down profile. Despite being averaged with the up profile, the higher concentrations near ground-level in the down profile caused a significant spike. The spike at 8:30 on 12/16/11 is attributable to trucks using the loading dock before and during the profile.

The urban canopy also plays an important role in the shape of the PNC profiles. The annex between the east and west buildings of PSI is 10 m high, and the south-to-north winds that prevail through the east and west buildings will mix and dilute particles emitted in the loading dock or along Paul Sullivan Way as seen in the 8:30 and 13:00 profiles in Figure 11 and the 9:00 profile in Figure 12. The PSI buildings are 24m tall, which is another height at which the particle count will be influenced by changing wind conditions. At this height the south-to-north winds that are typical in the urban canyon give way to the regional wind direction. In general, the buildings in cities lead to a more irregular flow field, resulting in greater mixing. Therefore, more mixing and more uniform concentration gradients will occur within the scale height of the buildings in a city than in a rural landscape.

Table 3: Summary Table of Vertical Profile Results

Date	Time	Wind Conditions ¹		Percent Change over the Profile ²		
		Direction	Speed (mph)	Temperature ³	PNC	PM2.5
12/16/2011	8:30 ⁴	W	20.6	4.5	-12.9	-36.5
	9:30	SSW	10.7	5.5	13.9	-16.7
	10:30	W	16.6	4.7	92.8	12.2
12/9/2011	12:00	SSW	11.4	0.5	-4.6	2.1
	13:00 ⁴	SSW	7.6	-4.6	-28.8	-15.8
	14:00	SSW	13.9	-9	19	-9.8
	15:00	SSW	11.0	0	9.6	NA
11/18/2011	15:30	W	9.4	0.5	13.7	13.9
	16:30	W	4.3	3.1	26.9	-0.4
	17:30	W	7.4	-1.8	-9.5	-8.9
3/15/2012	6:30	NE	4.5	-0.5	-13.5	-22.7
	7:15	NE	8.0	-5.5	-36.3	-21.8
	8:00	NE	6.5	-12.3	-59.5	-24.2
2/3/2012	9:00	NNW	5.0	-3	-7.4	-15.5
	10:00	NNW	9.0	6.4	-17.1	-25.2
	11:00	NW	5.5	-4.4	19.5	4.6
1/20/2012	12:00	WNW	8.1	-25.2	-31	5.5
	13:00	WNW	4.7	-34.3	-36.7	10.6
	14:00	WNW	7.4	-10.5	60.7	23.2
	15:00	WNW	6.5	-8.4	7.2	-2.8
2/15/2012	16:00	SSW	1.0	0.8	32.9	3.6
	17:00	Calm	Calm	1.3	-13.4	-6
	18:00	SSW	2.0	1.8	-13.1	1
Average			8.2	-3.9	0.5	-5.9
Standard Deviation			4.6	9.7	33.4	15.2

Notes:

1. Wind data on 2/3/12, 2/15/12, and 3/15/12 from the Winthrop Beach weather station, located 5 mi. east-northeast of PSI. Light winds from the east were observed at PSI on 2/15/12.

2. Percent change was calculated using: $\left(\frac{\mu_{30-35m}}{\mu_{1-6m}} \right) * 100 - 100$

3. Temperature profiles were adiabatically adjusted

4. 8:30 on 12/16/11 and 13:00 on 12/9/11 were affected by local sources (see Section 4.1.5)

4.4 Long-term Air Quality

The data from the stationary box on the roof of PSI provides a long-term representation of the air quality near I-93. Since the wind vane did not operate properly due to icing, the wind data has been supplemented with data from the Winthrop Beach weather station, located five miles east-northeast of PSI. This weather station is located outside of Boston and is not affected by the urban canopy; therefore, the wind measurements are representative of the coastal wind conditions in the region. Figure 17 shows the resulting wind rose and pollution rose using the wind data from Winthrop Beach and the particle count data from PSI. As expected, west to southwest winds predominate. Winds from the east were on average faster than those from the west. The pollution rose depicts higher concentrations at PSI during north and eastern winds (a greater percentage of light blue) compared to western winds (a greater percentage of yellow). This trend may reflect the impact of I-90 and I-93 on the particle counts at PSI over a longer timeframe.

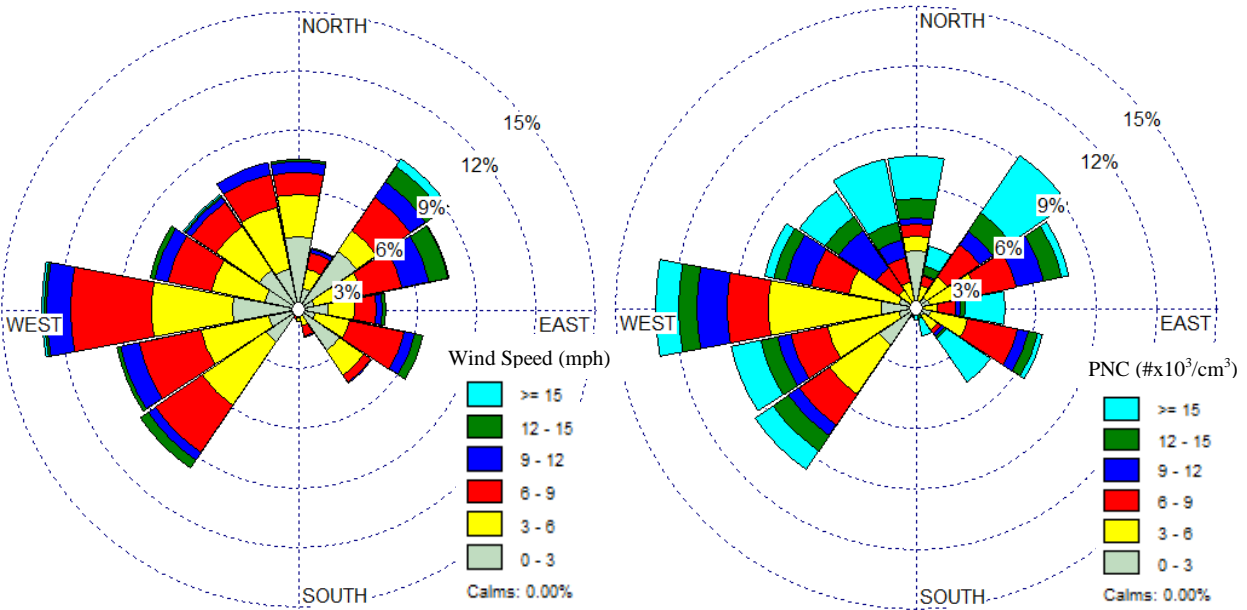


Figure 17: Wind roses showing the wind speed (left) and PNC (right) distributions that correspond with a particular wind direction from 1/21/12 to 2/9/12

PNC over the course of the day is dependent on the source strength, represented in Figure 18 by the traffic volume on I-93. The source strength follows a similar bimodal relationship with western winds because of the increased traffic volume across the city during morning and evening rush hours. The correlation between PNC and traffic volume breaks down slightly during the afternoon and evening rush hour. As the day progresses, the air above the earth heats up to an increasingly high altitude, raising the mixing height (Figure 3). The particles are more diluted as the day goes on, causing PNC to drop despite the increase in traffic in the evening. PNC also exhibits a dampened dependency on the traffic volume; although the traffic volume drops drastically at night, the concentrations only drop to approximately 50% of their peak value.

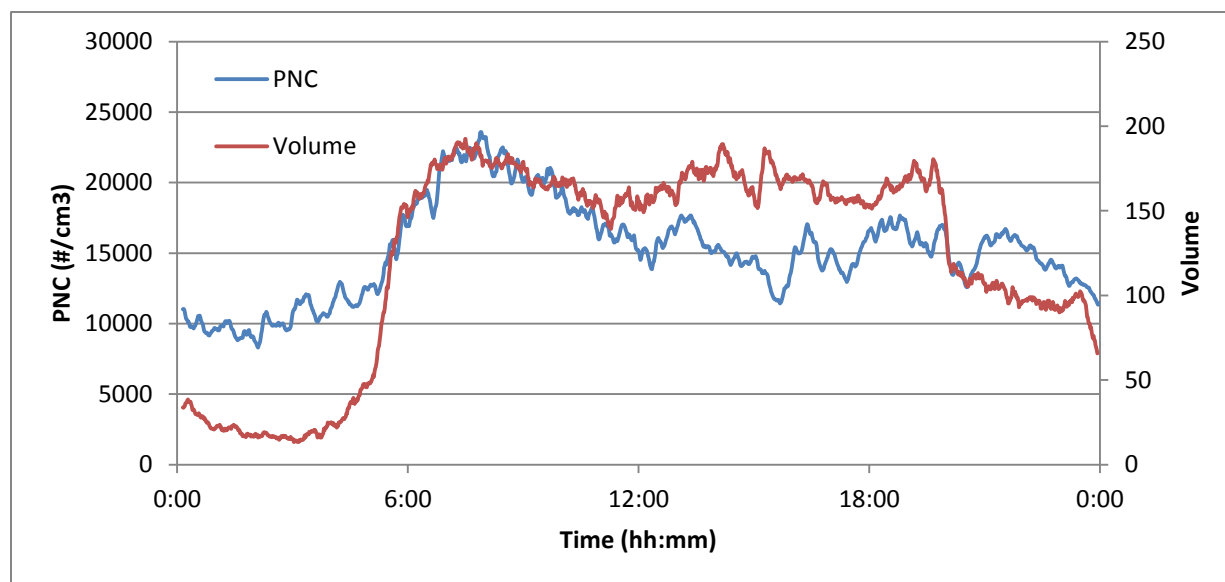


Figure 18: Average diurnal variation in PNC at PSI from 1/21/12 to 2/8/12 and traffic volume on I-93 on 2/3/12

Long-term trends in the vertical profiles emerge when analyzing the vertical profiles over the course of the entire sampling period. Both PNC and $PM_{2.5}$ demonstrate slight decreases with height when all the profiles are averaged together (Figure 19). This average reflects the long-term daytime concentration profiles since no profiles were collected at night. The percent decreases are small compared to the studies described in Section 1.2; approximately 6% for

PM_{2.5} and 8% for PNC. When the percent change of each profile is calculated first and then the changes averaged, the average percent change is approximately -6% for PM_{2.5} and 0.5% for PNC (Table 3). This method considers the percent change of each day individually, so that the relative magnitude of each profile is ignored. For example, a day when the concentration drops from 2000 #/cm³ to 1000 #/cm³ will have the same percent change as a day when the concentration drops from 10000 #/cm³ to 5000 #/cm³. Therefore, the decrease in the PNC in Figure 19 compared to the increase in Table 3 is driven by days with high concentrations when the concentrations drop off more than a low concentration day yet still have a smaller percent change. These poor air quality scenarios occur less often because of the infrequency of east winds, but they may be important from an exposure viewpoint (Figure 17).

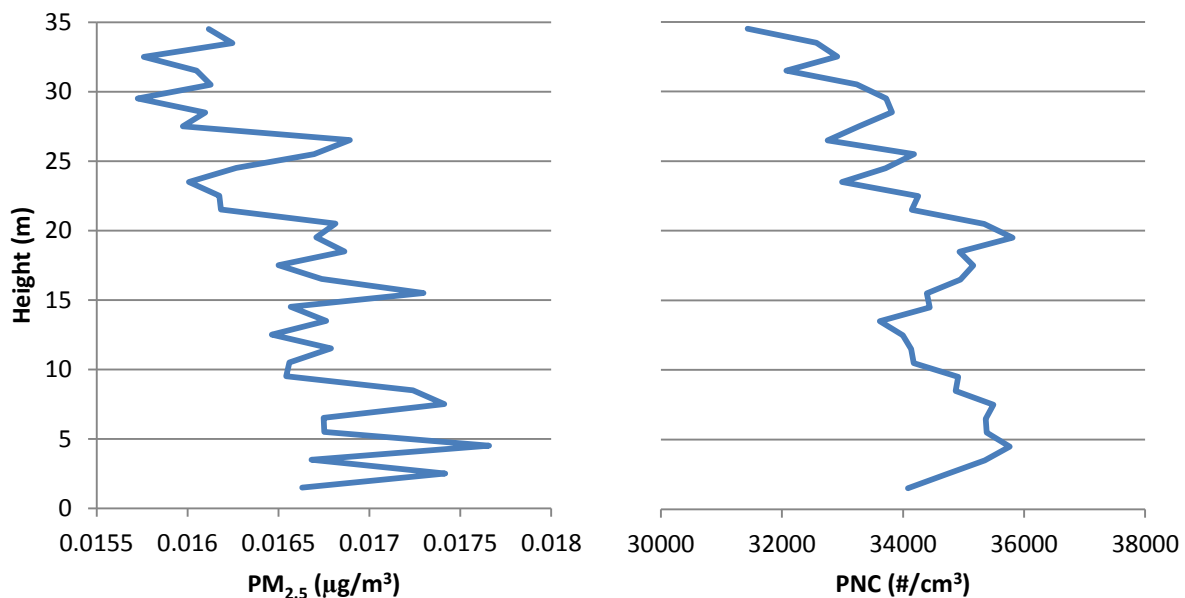


Figure 19: Average PM_{2.5} and PNC vertical profiles at PSI from 11/18/11 to 3/15/12 based on 23 profiles

5.0 CONCLUSIONS

This study measured vertical profiles of particulate matter in a near-highway environment. The impact of the highway and meteorological conditions on the slope and magnitude of the profiles were analyzed concurrently. The temperature profile, the wind direction, and the source strength were determined to be the most influential variables on the profiles. The temperature profile indicated the stability of the atmosphere and governed the vertical transport of the smaller particles that made up the particle count. The magnitude of PNC and the $PM_{2.5}$ concentration were dependent on the wind direction and source strength. The worst concentrations occurred downwind of the highway, especially during neutral or stable atmospheric conditions.

Compared to other studies on vertical profiles of particulate matter, PNC and the $PM_{2.5}$ concentration did not demonstrate a representative decrease in concentration with height. The $PM_{2.5}$ concentrations were independent of height, and the PNC profiles exhibited increases in concentration over the 35 m sampling height more often than decreases due to the extent of mixing within this layer. Over long periods of time, average PNC and $PM_{2.5}$ concentrations decrease slightly due to worse ground-level concentrations on poor air quality days; however, most of the time the exposure to particulates up to ten stories high is comparable to ground-level exposures and should not be dismissed as an exposure pathway.

REFERENCES

- Cooper, D.C. and Alley, F.C. (2002). "Air Pollution Control: A Design Approach," Waveland Press, Inc., Long Grove, Illinois.
- Environmental Protection Agency (1990). "The Clean Air Act." <http://www.epa.gov/air/caa/> (viewed April 23, 2012)
- Fuller, C.H., Zamore, W., Durant, J., Spengler, J., D. Brugge (2011). "Exposure to Highway-related Ultrafine Particles and Cardiovascular Markers: The CAFEH Project," *Epidemiology*, vol. 22, no. 1, pp. S227-S228.
- Jacob, D. J. (1999). "Introduction to Atmospheric Chemistry," Princeton University Press, Princeton, New Jersey.
- Kreyling, W.G., Semmler, M., Erbe, F., Oberdörster, G., Ziesenis, A., Mayer, P., Takenaka, S., and H. Schulz (2002). "Translocation of Ultrafine Insoluble Iridium Particles from Lung Epithelium to Extrapulmonary Organs is Size Dependent but Very Low," *Journal of Toxicology and Environmental Health, Part A*, no. 65, pp. 1513–1530.
- McKendry, I.G., Sturman, A.P., and J. Vergeiner (2004). "Vertical Profiles of Particulate Matter Size Distributions during Winter Domestic Burning in Christchurch, New Zealand," *Atmospheric Environment* vol. 38, pp. 4805–4813.
- Morawska, L., Thomas, S., Gilbert, D., Greenaway, C., and E. Rijnders (1999). "A Study of Horizontal and Vertical Profile of Submicrometer Particles in Relation to a Busy Road," *Atmospheric Environment*, vol. 33, pp. 1261–1274.
- Oberdörster, Günter, Eva Oberdörster, and Jan Oberdörster (2005). "Nanotoxicology: An Emerging Discipline Evolving from Studies of Ultrafine Particles," *Environmental Health Perspectives*, vol. 113, no. 7, pp. 823–838.
- Ratliff, G., Sequeira, C., Waitz, I., Ohsfeldt, M., Thrasher, T., Graham, M., and T. Thompson (2009). "Aircraft Impacts on Local and Regional Air Quality in the United States," PARTNER Project 15 final report.
- Seinfeld, J.H. and Pandis, S.N. (2007). "Atmospheric Chemistry and Physics: From Air Pollution to Climate Change," New York, John Wiley & Sons.
- Wu, Y., Hao, J., Fu, L., Wang, Z., and U. Tang (2002). "Vertical and Horizontal Profiles of Airborne Particulate Matter near Major Roads in Macao, China," *Atmospheric Environment*, vol. 36, pp. 4907–4918

- Zhang, K.M., Wexler, A.S., Zhu, Y., Hinds, W.C., and C. Sioutas (2004). "Evolution of Particle Number Distribution near Roadways Part II: the 'Road-to-Ambient' Process," *Atmospheric Environment* vol. 38, pp. 6655–6665.
- Zhu, Y. and Hinds, W.C. (2004). "Predicting Particle Number Concentration near a Highway based on Vertical Concentration Profile," *Atmospheric Environment* vol. 39, pp. 1557–1556
- Zhu, Y., Hinds, W.C., Kim, S., Shen, S., and C. Sioutas (2002). "Study of Ultrafine Particles near a Major Highway with Heavy-duty Diesel Traffic," *Atmospheric Environment* vol. 36, pp. 4323–4335.

APPENDIX A – Photo Log



Photo 1: View of the ladder to the floor 9. Instruments could not be transported past this point.

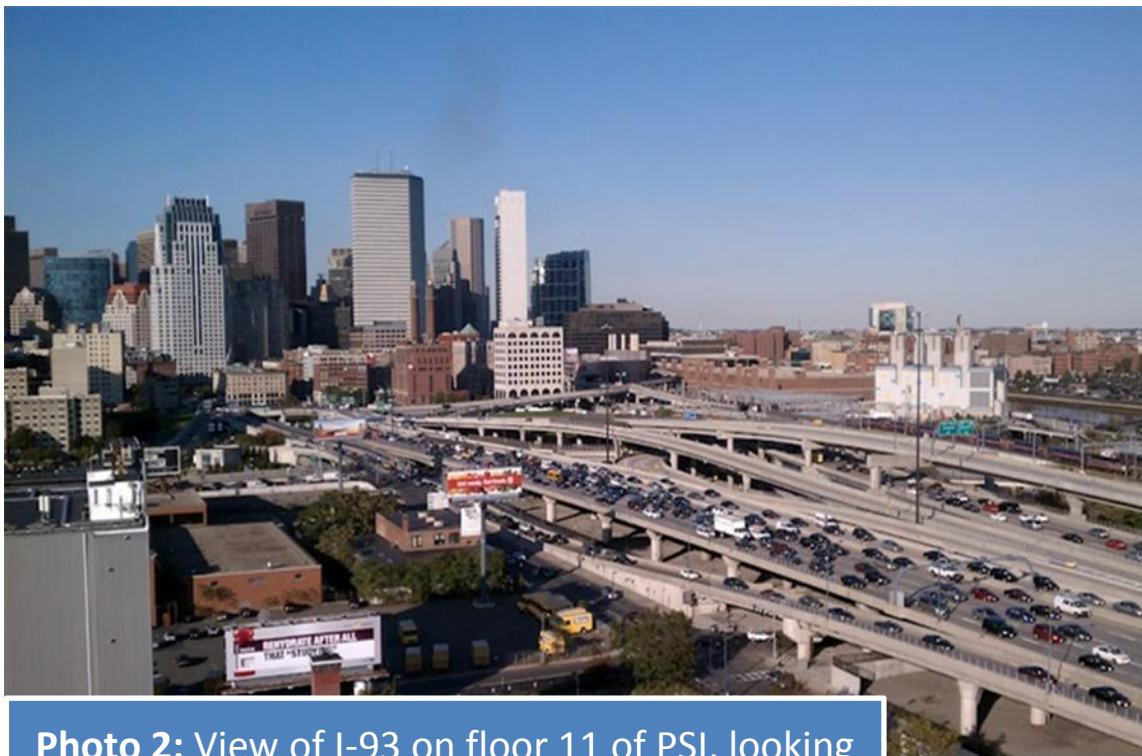


Photo 2: View of I-93 on floor 11 of PSI, looking northeast.

APPENDIX A – Photo Log



Photo 3: View of the pelican case mid-profile, looking down.

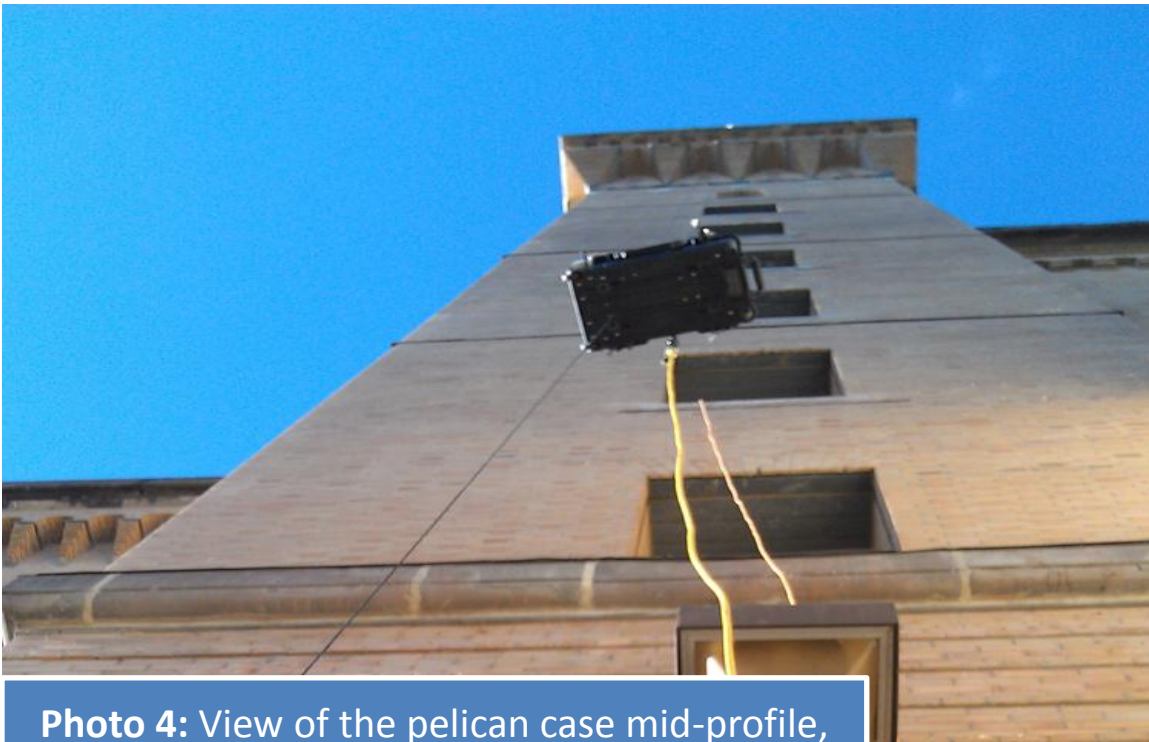


Photo 4: View of the pelican case mid-profile, looking up.

APPENDIX A – Photo Log



Photo 5: View of the weather balloon setup prior to collecting the profile.

Vertical Dispersion Monitoring Session Standard Operating Procedure

- 1. Order of operations**
 - a. Setup Pelican at Tufts**
 - i. CPC**
 1. Fill up the water tank with DI water (keep cap loose) and plug it in.
 2. Turn on CPC. Once it has warmed up, connect to laptop with the USB connection (COM4: USB port in bottom right), and go to File:3781 WCPC Import/Logging:Logging within the Aerosol Instrument Manager. Click on Start with the average interval at 1 sec.
 3. Within the same menu, synchronize CPC time with computer time. Close out of the program and unplug from the computer.
 4. Put CPC 709 in Pelican while running. Make sure there are no flow rate errors during this process.
 5. Turn off the CPC, put cap on inlet, unplug water tank and tighten cap, and pack into Pelican.
 - ii. HOBO Probe**
 1. Plug probe into USB port
 2. Open HOBOWare pro.
 3. Click on launch logger and set the logging interval to 1 second and set start logging to push button. Click start and unplug the probe. Clip onto exterior of Pelican. If it is precipitating, don't use the probe!
 - iii. Sidepak**
 1. Plug the Sidepak into COM4 and sync time with computer
 2. Clear memory (save data if necessary).
 3. Make sure it is fully charged
 - b. Pack Pelican and equipment into car. Go through checklist and check off items.**
 - c. Upon arrival at Pine Street Inn (PSI), set up pulley rig.**
 - i. The procedure for Person 1:**
 1. Carry items on checklist to the base of the tower (outside)
 2. Set up the instruments as described in **2**. Wait for the extension cord to set up the CPC.
 3. Hit the button on the TRH probe to begin collection.
 4. Once Person 2 has lowered the white rope, hook it onto the black rope. Uncoil the black rope while Person 2 hauls it up.
 5. Once the black rope is fed all the way down through the pulley, clip it on to the Pelican.
 6. Connect winch wires and ignition wire to electrodes with clips.
 7. Run the winch in until the Pelican is a few inches off the ground. Check to make sure the Pelican is level and secure and none of the ropes/cords are tangled.

APPENDIX B – Experimental Procedure

- ii. The procedure for Person 2:
 - 1. Carry items on checklist up the tower.
 - 2. On the 4th floor, plug in the extension cords and lower them out the window to Person 1.
 - 3. Proceed to the 9th floor (first floor outside) and set up the pulley system.
 - a. Tie the two pulley loops around the two crenellations facing the highway.
 - b. Feed the long white rope down to Person 1.
 - c. Pull the black rope up with the white rope. Untie the white rope from it, feed the black rope through the pulley such that the rope is heading down on the right side of the pulley, and let it back down to Person 1.
 - d. Make sure the electrical tape is against the concrete of the tower and not the rope.
 - d. At this point, the first profile is ready to be collected. Person 2 should join Person 1 on the ground floor. Leave all hatches and doors open. Person 1 should run the winch in so that the Pelican rises. Person 2 should record the time the profile begins, the time it gets to the top, and the time it ends. In addition, Person 2 should get the wind speed and the wind direction on the roof and record it in the data log (if necessary). The side of the tower facing towards the highway is oriented ESE.
 - e. Once the top of the tower has been reached, run the winch out to return it to the ground.
 - f. Repeat steps **1d.-f.** every half hour.
2. Setting up equipment and Data Collection
- a. Sidepak
 - i. Turn on device and let warm up.
 - ii. Calibrate sidepack
 - 1. Attach zero filter and zero the device by selecting Zero Cal in the main menu.
 - 2. Wait 60 seconds for calibration to complete
 - iii. Set the collection interval to 10 second
 - 1. Select setup-loginterval-logintvl 1
 - iv. Take flow measurement using burst setting on flow meter
 - v. Select data log – run manual. Collect data for 5 minutes. Record start and end time (instrument it recording data when it says “logging data”).
 - vi. Press back arrow to stop test
 - b. CPC (708)
 - i. Plug water tank into CPC and attach inlet tubing.

APPENDIX B – *Experimental Procedure*

- - Plug in instrument and wait 10 minutes for it to warm up. The display will stop displaying a hyphen when it's warm.
 - Make sure water cap is loose, inlet cap is off, and pump is on.
 - Use the calibration tube to test the precision of CPC.
 - Take flow measurement using burst setting on flow meter
- Anemometer (if necessary)
 - With the wrist-strap on, collect and record wind speed (m/s) and direction measurements on the roof of the building during each profile.
 - Record time and value of each measurement.

3. Data Upload

a. Sidepak

- i.** When back at tufts, plug Sidepak into COM5 (front right USB). Open TrakPro and click receive in the file menu.
- ii.** Select all samples from the days monitoring session to download.
- iii.** Save the file as a TrakPro data file in the PM25 folder called mmddyyyy and as an excel file (export data as comma delimited) in the folder of that day of logging called mmddyyyy PM25.

b. CPC (708)

- i.** Upon returning to Tufts, connect the CPC to the laptop via the USB connection (COM4: bottom right USB port).
- ii.** Select file:3781 WCPC Import/Logging:Logging:Stop
- iii.** Click exit and then read memory.
- iv.** Click save as:text file for the files during the monitoring period. Save them as mmddyyyy in the PNC raw data folder.
- v.** Open the files, comma delimit the data, paste them into one file, and resave as an excel workbook under a new folder for that day of logging called mmddyyyy PNC.
- vi.** Once the data has been transferred onto your computer, delete the txt file and the data from the memory drive. Within the Import/Logging menu, click on Logging:Clear Memory.

c. Temperature and Relative Humidity

- i.** When back at Tufts, plug in probe to USB port and open HOBOWare pro. Click read out and save the file as mmddyyyy in the Temp and RH raw data folder.
- ii.** Click plot when prompted. After the output is displayed click export table data and click export. Save the file as mmddyyyy TRH in the folder for that day of logging.

4. Take Down

APPENDIX B – *Experimental Procedure*

- a.** CPC (708)
 - i.** Empty out water tank.
 - ii.** Run CPC with the water tank below the CPC to drain it for an hour.
 - iii.** Pack it with the other WCPC.
- b.** Copy the folder for that day of logging onto r-drive and dropbox.

Tower Height		Profile								
	1	2								
Entry	Data	Up		Down		Data	Up		Down	
	Height	Data	Height	Data	Height	Data	Height	Data	Height	
34										
1	=z*\$A5/COUNT(B\$4:B\$430)	=z-z*(SA5-1)/COUNT(D\$4:D\$430)	=z*\$A5/COUNT(F\$4:F\$430)	=z-z*(SA5-1)/COUNT(H\$4:H\$430)						
2	=z*\$A6/COUNT(B\$4:B\$430)	=z-z*(SA6-1)/COUNT(D\$4:D\$430)	=z*\$A6/COUNT(F\$4:F\$430)	=z-z*(SA6-1)/COUNT(H\$4:H\$430)						
3	=z*\$A7/COUNT(B\$4:B\$430)	=z-z*(SA7-1)/COUNT(D\$4:D\$430)	=z*\$A7/COUNT(F\$4:F\$430)	=z-z*(SA7-1)/COUNT(H\$4:H\$430)						
4	=z*\$A8/COUNT(B\$4:B\$430)	=z-z*(SA8-1)/COUNT(D\$4:D\$430)	=z*\$A8/COUNT(F\$4:F\$430)	=z-z*(SA8-1)/COUNT(H\$4:H\$430)						
5	=z*\$A9/COUNT(B\$4:B\$430)	=z-z*(SA9-1)/COUNT(D\$4:D\$430)	=z*\$A9/COUNT(F\$4:F\$430)	=z-z*(SA9-1)/COUNT(H\$4:H\$430)						
6	=z*\$A10/COUNT(B\$4:B\$430)	=z-z*(SA10-1)/COUNT(D\$4:D\$430)	=z*\$A10/COUNT(F\$4:F\$430)	=z-z*(SA10-1)/COUNT(H\$4:H\$430)						
7	=z*\$A11/COUNT(B\$4:B\$430)	=z-z*(SA11-1)/COUNT(D\$4:D\$430)	=z*\$A11/COUNT(F\$4:F\$430)	=z-z*(SA11-1)/COUNT(H\$4:H\$430)						
8	=z*\$A12/COUNT(B\$4:B\$430)	=z-z*(SA12-1)/COUNT(D\$4:D\$430)	=z*\$A12/COUNT(F\$4:F\$430)	=z-z*(SA12-1)/COUNT(H\$4:H\$430)						
9	=z*\$A13/COUNT(B\$4:B\$430)	=z-z*(SA13-1)/COUNT(D\$4:D\$430)	=z*\$A13/COUNT(F\$4:F\$430)	=z-z*(SA13-1)/COUNT(H\$4:H\$430)						
10	=z*\$A14/COUNT(B\$4:B\$430)	=z-z*(SA14-1)/COUNT(D\$4:D\$430)	=z*\$A14/COUNT(F\$4:F\$430)	=z-z*(SA14-1)/COUNT(H\$4:H\$430)						
11	=z*\$A15/COUNT(B\$4:B\$430)	=z-z*(SA15-1)/COUNT(D\$4:D\$430)	=z*\$A15/COUNT(F\$4:F\$430)	=z-z*(SA15-1)/COUNT(H\$4:H\$430)						
12	=z*\$A16/COUNT(B\$4:B\$430)	=z-z*(SA16-1)/COUNT(D\$4:D\$430)	=z*\$A16/COUNT(F\$4:F\$430)	=z-z*(SA16-1)/COUNT(H\$4:H\$430)						
13	=z*\$A17/COUNT(B\$4:B\$430)	=z-z*(SA17-1)/COUNT(D\$4:D\$430)	=z*\$A17/COUNT(F\$4:F\$430)	=z-z*(SA17-1)/COUNT(H\$4:H\$430)						
14	=z*\$A18/COUNT(B\$4:B\$430)	=z-z*(SA18-1)/COUNT(D\$4:D\$430)	=z*\$A18/COUNT(F\$4:F\$430)	=z-z*(SA18-1)/COUNT(H\$4:H\$430)						
15	=z*\$A19/COUNT(B\$4:B\$430)	=z-z*(SA19-1)/COUNT(D\$4:D\$430)	=z*\$A19/COUNT(F\$4:F\$430)	=z-z*(SA19-1)/COUNT(H\$4:H\$430)						
16	=z*\$A20/COUNT(B\$4:B\$430)	=z-z*(SA20-1)/COUNT(D\$4:D\$430)	=z*\$A20/COUNT(F\$4:F\$430)	=z-z*(SA20-1)/COUNT(H\$4:H\$430)						
17	=z*\$A21/COUNT(B\$4:B\$430)	=z-z*(SA21-1)/COUNT(D\$4:D\$430)	=z*\$A21/COUNT(F\$4:F\$430)	=z-z*(SA21-1)/COUNT(H\$4:H\$430)						
18	=z*\$A22/COUNT(B\$4:B\$430)	=z-z*(SA22-1)/COUNT(D\$4:D\$430)	=z*\$A22/COUNT(F\$4:F\$430)	=z-z*(SA22-1)/COUNT(H\$4:H\$430)						
19	=z*\$A23/COUNT(B\$4:B\$430)	=z-z*(SA23-1)/COUNT(D\$4:D\$430)	=z*\$A23/COUNT(F\$4:F\$430)	=z-z*(SA23-1)/COUNT(H\$4:H\$430)						
20	=z*\$A24/COUNT(B\$4:B\$430)	=z-z*(SA24-1)/COUNT(D\$4:D\$430)	=z*\$A24/COUNT(F\$4:F\$430)	=z-z*(SA24-1)/COUNT(H\$4:H\$430)						
21	=z*\$A25/COUNT(B\$4:B\$430)	=z-z*(SA25-1)/COUNT(D\$4:D\$430)	=z*\$A25/COUNT(F\$4:F\$430)	=z-z*(SA25-1)/COUNT(H\$4:H\$430)						
22	=z*\$A26/COUNT(B\$4:B\$430)	=z-z*(SA26-1)/COUNT(D\$4:D\$430)	=z*\$A26/COUNT(F\$4:F\$430)	=z-z*(SA26-1)/COUNT(H\$4:H\$430)						
23	=z*\$A27/COUNT(B\$4:B\$430)	=z-z*(SA27-1)/COUNT(D\$4:D\$430)	=z*\$A27/COUNT(F\$4:F\$430)	=z-z*(SA27-1)/COUNT(H\$4:H\$430)						
24	=z*\$A28/COUNT(B\$4:B\$430)	=z-z*(SA28-1)/COUNT(D\$4:D\$430)	=z*\$A28/COUNT(F\$4:F\$430)	=z-z*(SA28-1)/COUNT(H\$4:H\$430)						
25	=z*\$A29/COUNT(B\$4:B\$430)	=z-z*(SA29-1)/COUNT(D\$4:D\$430)	=z*\$A29/COUNT(F\$4:F\$430)	=z-z*(SA29-1)/COUNT(H\$4:H\$430)						
26	=z*\$A30/COUNT(B\$4:B\$430)	=z-z*(SA30-1)/COUNT(D\$4:D\$430)	=z*\$A30/COUNT(F\$4:F\$430)	=z-z*(SA30-1)/COUNT(H\$4:H\$430)						
27	=z*\$A31/COUNT(B\$4:B\$430)	=z-z*(SA31-1)/COUNT(D\$4:D\$430)	=z*\$A31/COUNT(F\$4:F\$430)	=z-z*(SA31-1)/COUNT(H\$4:H\$430)						
28	=z*\$A32/COUNT(B\$4:B\$430)	=z-z*(SA32-1)/COUNT(D\$4:D\$430)	=z*\$A32/COUNT(F\$4:F\$430)	=z-z*(SA32-1)/COUNT(H\$4:H\$430)						
29	=z*\$A33/COUNT(B\$4:B\$430)	=z-z*(SA33-1)/COUNT(D\$4:D\$430)	=z*\$A33/COUNT(F\$4:F\$430)	=z-z*(SA33-1)/COUNT(H\$4:H\$430)						
30	=z*\$A34/COUNT(B\$4:B\$430)	=z-z*(SA34-1)/COUNT(D\$4:D\$430)	=z*\$A34/COUNT(F\$4:F\$430)	=z-z*(SA34-1)/COUNT(H\$4:H\$430)						
31	=z*\$A35/COUNT(B\$4:B\$430)	=z-z*(SA35-1)/COUNT(D\$4:D\$430)	=z*\$A35/COUNT(F\$4:F\$430)	=z-z*(SA35-1)/COUNT(H\$4:H\$430)						
32	=z*\$A36/COUNT(B\$4:B\$430)	=z-z*(SA36-1)/COUNT(D\$4:D\$430)	=z*\$A36/COUNT(F\$4:F\$430)	=z-z*(SA36-1)/COUNT(H\$4:H\$430)						
33	=z*\$A37/COUNT(B\$4:B\$430)	=z-z*(SA37-1)/COUNT(D\$4:D\$430)	=z*\$A37/COUNT(F\$4:F\$430)	=z-z*(SA37-1)/COUNT(H\$4:H\$430)						
34	=z*\$A38/COUNT(B\$4:B\$430)	=z-z*(SA38-1)/COUNT(D\$4:D\$430)								

APPENDIX C – Example PNC Data Sheet and Macro Code

Profile										Spatial Averages				
3		4		4		3		2		1				
Up		Down		Up		Down								Height
Data	Height	Data	Height	Data	Height	Data	Height	Enter Time	Enter Time	Enter Time	Enter Time	Enter Time	Enter Time	
	=Z*\$A5/(COUNT(\$A:\$A30))		=Z-Z*(\$A5-1)/(COUNT(\$A:\$A30))		=Z*\$5/(COUNT(\$N:\$N430))		=Z-Z*(\$A5-1)/(COUNT(\$P\$4:\$P\$430))							1.5
	=Z*\$A6/(COUNT(\$A:\$A30))		=Z-Z*(\$A6-1)/(COUNT(\$A:\$A30))		=Z*\$A6/(COUNT(\$N:\$N430))		=Z-Z*(\$A6-1)/(COUNT(\$P\$4:\$P\$430))							2.5
	=Z*\$A7/(COUNT(\$A:\$A30))		=Z-Z*(\$A7-1)/(COUNT(\$A:\$A30))		=Z*\$A7/(COUNT(\$N:\$N430))		=Z-Z*(\$A7-1)/(COUNT(\$P\$4:\$P\$430))							3.5
	=Z*\$A8/(COUNT(\$A:\$A30))		=Z-Z*(\$A8-1)/(COUNT(\$A:\$A30))		=Z*\$A8/(COUNT(\$N:\$N430))		=Z-Z*(\$A8-1)/(COUNT(\$P\$4:\$P\$430))							4.5
	=Z*\$A9/(COUNT(\$A:\$A30))		=Z-Z*(\$A9-1)/(COUNT(\$A:\$A30))		=Z*\$A9/(COUNT(\$N:\$N430))		=Z-Z*(\$A9-1)/(COUNT(\$P\$4:\$P\$430))							5.5
	=Z*\$A10/(COUNT(\$A:\$A30))		=Z-Z*(\$A10-1)/(COUNT(\$A:\$A30))		=Z*\$A10/(COUNT(\$N:\$N430))		=Z-Z*(\$A10-1)/(COUNT(\$P\$4:\$P\$430))							6.5
	=Z*\$A11/(COUNT(\$A:\$A30))		=Z-Z*(\$A11-1)/(COUNT(\$A:\$A30))		=Z*\$A11/(COUNT(\$N:\$N430))		=Z-Z*(\$A11-1)/(COUNT(\$P\$4:\$P\$430))							7.5
	=Z*\$A12/(COUNT(\$A:\$A30))		=Z-Z*(\$A12-1)/(COUNT(\$A:\$A30))		=Z*\$A12/(COUNT(\$N:\$N430))		=Z-Z*(\$A12-1)/(COUNT(\$P\$4:\$P\$430))							8.5
	=Z*\$A13/(COUNT(\$A:\$A30))		=Z-Z*(\$A13-1)/(COUNT(\$A:\$A30))		=Z*\$A13/(COUNT(\$N:\$N430))		=Z-Z*(\$A13-1)/(COUNT(\$P\$4:\$P\$430))							9.5
	=Z*\$A14/(COUNT(\$A:\$A30))		=Z-Z*(\$A14-1)/(COUNT(\$A:\$A30))		=Z*\$A14/(COUNT(\$N:\$N430))		=Z-Z*(\$A14-1)/(COUNT(\$P\$4:\$P\$430))							10.5
	=Z*\$A15/(COUNT(\$A:\$A30))		=Z-Z*(\$A15-1)/(COUNT(\$A:\$A30))		=Z*\$A15/(COUNT(\$N:\$N430))		=Z-Z*(\$A15-1)/(COUNT(\$P\$4:\$P\$430))							11.5
	=Z*\$A16/(COUNT(\$A:\$A30))		=Z-Z*(\$A16-1)/(COUNT(\$A:\$A30))		=Z*\$A16/(COUNT(\$N:\$N430))		=Z-Z*(\$A16-1)/(COUNT(\$P\$4:\$P\$430))							12.5
	=Z*\$A17/(COUNT(\$A:\$A30))		=Z-Z*(\$A17-1)/(COUNT(\$A:\$A30))		=Z*\$A17/(COUNT(\$N:\$N430))		=Z-Z*(\$A17-1)/(COUNT(\$P\$4:\$P\$430))							13.5
	=Z*\$A18/(COUNT(\$A:\$A30))		=Z-Z*(\$A18-1)/(COUNT(\$A:\$A30))		=Z*\$A18/(COUNT(\$N:\$N430))		=Z-Z*(\$A18-1)/(COUNT(\$P\$4:\$P\$430))							14.5
	=Z*\$A19/(COUNT(\$A:\$A30))		=Z-Z*(\$A19-1)/(COUNT(\$A:\$A30))		=Z*\$A19/(COUNT(\$N:\$N430))		=Z-Z*(\$A19-1)/(COUNT(\$P\$4:\$P\$430))							15.5
	=Z*\$A20/(COUNT(\$A:\$A30))		=Z-Z*(\$A20-1)/(COUNT(\$A:\$A30))		=Z*\$A20/(COUNT(\$N:\$N430))		=Z-Z*(\$A20-1)/(COUNT(\$P\$4:\$P\$430))							16.5
	=Z*\$A21/(COUNT(\$A:\$A30))		=Z-Z*(\$A21-1)/(COUNT(\$A:\$A30))		=Z*\$A21/(COUNT(\$N:\$N430))		=Z-Z*(\$A21-1)/(COUNT(\$P\$4:\$P\$430))							17.5
	=Z*\$A22/(COUNT(\$A:\$A30))		=Z-Z*(\$A22-1)/(COUNT(\$A:\$A30))		=Z*\$A22/(COUNT(\$N:\$N430))		=Z-Z*(\$A22-1)/(COUNT(\$P\$4:\$P\$430))							18.5
	=Z*\$A23/(COUNT(\$A:\$A30))		=Z-Z*(\$A23-1)/(COUNT(\$A:\$A30))		=Z*\$A23/(COUNT(\$N:\$N430))		=Z-Z*(\$A23-1)/(COUNT(\$P\$4:\$P\$430))							19.5
	=Z*\$A24/(COUNT(\$A:\$A30))		=Z-Z*(\$A24-1)/(COUNT(\$A:\$A30))		=Z*\$A24/(COUNT(\$N:\$N430))		=Z-Z*(\$A24-1)/(COUNT(\$P\$4:\$P\$430))							20.5
	=Z*\$A25/(COUNT(\$A:\$A30))		=Z-Z*(\$A25-1)/(COUNT(\$A:\$A30))		=Z*\$A25/(COUNT(\$N:\$N430))		=Z-Z*(\$A25-1)/(COUNT(\$P\$4:\$P\$430))							21.5
	=Z*\$A26/(COUNT(\$A:\$A30))		=Z-Z*(\$A26-1)/(COUNT(\$A:\$A30))		=Z*\$A26/(COUNT(\$N:\$N430))		=Z-Z*(\$A26-1)/(COUNT(\$P\$4:\$P\$430))							22.5
	=Z*\$A27/(COUNT(\$A:\$A30))		=Z-Z*(\$A27-1)/(COUNT(\$A:\$A30))		=Z*\$A27/(COUNT(\$N:\$N430))		=Z-Z*(\$A27-1)/(COUNT(\$P\$4:\$P\$430))							23.5
	=Z*\$A28/(COUNT(\$A:\$A30))		=Z-Z*(\$A28-1)/(COUNT(\$A:\$A30))		=Z*\$A28/(COUNT(\$N:\$N430))		=Z-Z*(\$A28-1)/(COUNT(\$P\$4:\$P\$430))							24.5
	=Z*\$A29/(COUNT(\$A:\$A30))		=Z-Z*(\$A29-1)/(COUNT(\$A:\$A30))		=Z*\$A29/(COUNT(\$N:\$N430))		=Z-Z*(\$A29-1)/(COUNT(\$P\$4:\$P\$430))							25.5
	=Z*\$A30/(COUNT(\$A:\$A30))		=Z-Z*(\$A30-1)/(COUNT(\$A:\$A30))		=Z*\$A30/(COUNT(\$N:\$N430))		=Z-Z*(\$A30-1)/(COUNT(\$P\$4:\$P\$430))							26.5
	=Z*\$A31/(COUNT(\$A:\$A30))		=Z-Z*(\$A31-1)/(COUNT(\$A:\$A30))		=Z*\$A31/(COUNT(\$N:\$N430))		=Z-Z*(\$A31-1)/(COUNT(\$P\$4:\$P\$430))							27.5
	=Z*\$A32/(COUNT(\$A:\$A30))		=Z-Z*(\$A32-1)/(COUNT(\$A:\$A30))		=Z*\$A32/(COUNT(\$N:\$N430))		=Z-Z*(\$A32-1)/(COUNT(\$P\$4:\$P\$430))							28.5
	=Z*\$A33/(COUNT(\$A:\$A30))		=Z-Z*(\$A33-1)/(COUNT(\$A:\$A30))		=Z*\$A33/(COUNT(\$N:\$N430))		=Z-Z*(\$A33-1)/(COUNT(\$P\$4:\$P\$430))							29.5
	=Z*\$A34/(COUNT(\$A:\$A30))		=Z-Z*(\$A34-1)/(COUNT(\$A:\$A30))		=Z*\$A34/(COUNT(\$N:\$N430))		=Z-Z*(\$A34-1)/(COUNT(\$P\$4:\$P\$430))							30.5
	=Z*\$A35/(COUNT(\$A:\$A30))		=Z-Z*(\$A35-1)/(COUNT(\$A:\$A30))		=Z*\$A35/(COUNT(\$N:\$N430))		=Z-Z*(\$A35-1)/(COUNT(\$P\$4:\$P\$430))							31.5
	=Z*\$A36/(COUNT(\$A:\$A30))		=Z-Z*(\$A36-1)/(COUNT(\$A:\$A30))		=Z*\$A36/(COUNT(\$N:\$N430))		=Z-Z*(\$A36-1)/(COUNT(\$P\$4:\$P\$430))							32.5
	=Z*\$A37/(COUNT(\$A:\$A30))		=Z-Z*(\$A37-1)/(COUNT(\$A:\$A30))		=Z*\$A37/(COUNT(\$N:\$N430))		=Z-Z*(\$A37-1)/(COUNT(\$P\$4:\$P\$430))							33.5
	=Z*\$A38/(COUNT(\$A:\$A30))		=Z-Z*(\$A38-1)/(COUNT(\$A:\$A30))		=Z*\$A38/(COUNT(\$N:\$N430))		=Z-Z*(\$A38-1)/(COUNT(\$P\$4:\$P\$430))							34.5
	=Z*\$A39/(COUNT(\$A:\$A30))		=Z-Z*(\$A39-1)/(COUNT(\$A:\$A30))		=Z*\$A39/(COUNT(\$N:\$N430))		=Z-Z*(\$A39-1)/(COUNT(\$P\$4:\$P\$430))							
	=Z*\$A40/(COUNT(\$A:\$A30))		=Z-Z*(\$A40-1)/(COUNT(\$A:\$A30))		=Z*\$A40/(COUNT(\$N:\$N430))		=Z-Z*(\$A40-1)/(COUNT(\$P\$4:\$P\$430))							
	=Z*\$A41/(COUNT(\$A:\$A30))		=Z-Z*(\$A41-1)/(COUNT(\$A:\$A30))		=Z*\$A41/(COUNT(\$N:\$N430))		=Z-Z*(\$A41-1)/(COUNT(\$P\$4:\$P\$430))							
	=Z*\$A42/(COUNT(\$A:\$A30))		=Z-Z*(\$A42-1)/(COUNT(\$A:\$A30))		=Z*\$A42/(COUNT(\$N:\$N430))		=Z-Z*(\$A42-1)/(COUNT(\$P\$4:\$P\$430))							
	=Z*\$A43/(COUNT(\$A:\$A30))		=Z-Z*(\$A43-1)/(COUNT(\$A:\$A30))		=Z*\$A43/(COUNT(\$N:\$N430))		=Z-Z*(\$A43-1)/(COUNT(\$P\$4:\$P\$430))							
	=Z*\$A44/(COUNT(\$A:\$A30))		=Z-Z*(\$A44-1)/(COUNT(\$A:\$A30))		=Z*\$A44/(COUNT(\$N:\$N430))		=Z-Z*(\$A44-1)/(COUNT(\$P\$4:\$P\$430))							
	=Z*\$A45/(COUNT(\$A:\$A30))		=Z-Z*(\$A45-1)/(COUNT(\$A:\$A30))		=Z*\$A45/(COUNT(\$N:\$N430))		=Z-Z*(\$A45-1)/(COUNT(\$P\$4:\$P\$430))							

APPENDIX C – Example PNC Data Sheet and Macro Code

Sub SpatialAveraging()
'Spatial Averaging of Vertical Profiles
'Written by Piers MacNaughton
'Last updated 11/19/2011

Application.ScreenUpdating = False
Sheets("Analysis").Select

'Define Variables

Dim i As Integer
Dim j As Integer
Dim k As Integer
Dim profile As Integer
Dim sumUp As Double
Dim sumDown As Double
Dim countup As Integer
Dim countdown As Integer
Dim avgup As Double
Dim avgdown As Double
Dim height As Double
Dim towerheight As Integer

profile = 0
towerheight = Range("A2").Value

'For loop that cycles through each profile

For profile = 0 To 3

 j = 0

 k = 0

 'For loop that cycles through each meter interval

 For i = 0 To towerheight - 1

 sumUp = 0

 sumDown = 0

 height = 0.5 + i

 Range("B5").Select

 ActiveCell.Offset(0, 4 * profile).Select

 Do

 countup = 0

 countdown = 0

 Do

 'If value is not in interval, proceed to next cell

 If ActiveCell.Offset(0, 1).Value <= (height - 0.5) Then

 ActiveCell.Offset(1, 0).Select

 Else

 'If value is in interval, add it to others in interval

 sumUp = sumUp + ActiveCell.Value

APPENDIX C – Example PNC Data Sheet and Macro Code

```
countup = countup + 1
ActiveCell.Offset(1, 0).Select
End If
'When the height exceeds the upper bound of interval, stop do loop
Loop Until ActiveCell.Offset(0, 1) > (height + 0.5) Or countup = 25
Range("D5").Select
ActiveCell.Offset(0, 4 * profile).Select
'Repeat process for the down profile, starting at the bottom
Do
    If ActiveCell.Offset(0, 1).Value > (height + 0.5) Then
        ActiveCell.Offset(1, 0).Select
    Else
        sumDown = sumDown + ActiveCell.Value
        countdown = countdown + 1
        ActiveCell.Offset(1, 0).Select
    End If
Loop Until ActiveCell.Offset(0, 1) <= (height - 0.5) Or countdown = 25
'Ends program if the number of cells summed is unexplainably large
If countup = 25 Or countdown = 25 Then
    End
End If
'Average the values in each bin
avgup = sumUp / countup
avgdown = sumDown / countdown
Range("U5").Select
'Average the up and down profile values and put in spatial averages table
ActiveCell.Offset(i, -profile).Value = (avgup + avgdown) / 2
Loop Until avgdown <> 0
Next i
Next profile
Application.ScreenUpdating = True
End Sub
```